Kinematic and paleomagnetic restoration of the Semail Ophiolite (Oman) reveals subduction initiation along an ancient Neotethyan fracture zone

Van Hinsbergen, Douwe J.J.; Maffione, Marco; Koornneef, Louise M T; Guilmette, Carl

DOI:
10.1016/j.epsl.2019.04.038

Elsevier Editorial System(tm) for Earth and Planetary Science Letters

Manuscript Draft

Manuscript Number:

Title: Kinematic and paleomagnetic restoration of the Semail Ophiolite (Oman) reveals subduction initiation along an ancient Neotethyan fracture zone

Article Type: Letters

Keywords: Paleomagnetism, Ophiolite, Plate reconstruction, kinematics, subduction, Neotethys

Corresponding Author: Dr. Douwe J.J. van Hinsbergen,

Corresponding Author's Institution: Utrecht University

First Author: Douwe J.J. van Hinsbergen

Order of Authors: Douwe J.J. van Hinsbergen; Marco Maffione; Louise Koornneef; Carl Guilmette

Abstract: The archetypal Semail ophiolite of Oman has inspired much thought on the dynamics of initiation of intra-oceanic subduction zones. Current models invoke subduction initiation at a mid-oceanic ridge located sufficiently close to the Arabian passive margin to allow initiation of continental subduction below the ophiolite within ~10-15 Myr after the 96-95 Ma age of formation of supra-subduction zone crust. Here, we perform an extensive paleomagnetic analysis of sheeted dyke sections across the Semail ophiolite to restore the orientation of the supra-subduction zone ridge during spreading. Our results consistently indicate that the ridge was oriented NNE-SSW, and we infer that the associated trench, close to the modern obduction front, had the same orientation. Our data are consistent with a previously documented ~150° clockwise rotation of the ophiolite, and we reconstruct that the original subduction zone was WNW-ward dipping and NNE-SSW striking. Initial subduction likely occurred in the ocean adjacent and parallel to the Arabian transform margin that formed the original underpinnings of rocks in the Zagros fold-thrust belt, now underthrust below Iran. Subduction thus likely initiated along an ancient, continental margin-parallel fracture zone, as also recently inferred from near-coeval ophiolites from the eastern Mediterranean and NW Arabian regions. Subduction initiation was therefore likely induced by (WN)W-(ES)E contraction, and this constraint may help the future identification of the dynamic triggers of Neotethyan subduction initiation in the Late Cretaceous.

Suggested Reviewers: Tony Morris
A.Morris@plymouth.ac.uk
Paleomagnetism, specialist on ophiolite paleomagnetism

Mathieu Soret
mathieu.soret@ubc.ca
Specialist on Oman ophiolite geology

Stephane Guillot

stephane.guillot@ujf-grenoble.fr
Specialist on structural geology and ophiolite geology

Laurent Jolivet
laurent.jolivet@univ-orleans.fr
Specilialist on tectonics and geodynamics

Bob Stern
rjstern@utdallas.edu
Specialist on subduction initiation and ophiolite geology

Opposed Reviewers:

Research Data Related to this Submission

Title: Data for: Kinematic and paleomagnetic restoration of the Semail Ophiolite (Oman) reveals subduction initiation along an ancient Neotethyan fracture zone
Repository: Mendeley Data
https://data.mendeley.com/datasets/35g6bmk6d3/draft?a=f0f49b1c-85d0-4623-b8f1-a6e3190ff254

Utrecht, January 2, 2019

Dear editor, dear An,

Hereby we resubmit our paper entitled 'Kinematic and paleomagnetic restoration of the Semail Ophiolite (Oman) reveals subduction initiation along an ancient Neotethyan fracture zone'.

Given the three negative reviews you received on this paper, we understand that you had no choice but to reject our paper. We welcome your kind invitation to resubmit after revision, and provide a detailed rebuttal to the reviews below.

Our paper received three reviews. The third reviewer is the only one who discusses the data we present and some of the kinematic interpretations based on those. This reviewer provided several detailed comments on the paleomagnetic data section that we have addressed in the revised version. This reviewer also argued that a very different interpretation is permitted – the counterclockwise net rotations which would yield more E-W trending dykes – and asked us for data allowing to discern between these. We will show below that those data were already provided, and that both modern structure as well as a large, previously published, and already cited paleomagnetic analysis on vertical axis rotations conclusively excludes the alternative perceived by the reviewer. This was already included in the original paper, and further clarified here.

The reviewer also speculates that the major rotations obtained here and previously could be explained by 'local deformation'. As we will explain below, and in more detail in the revised manuscript, the Oman ophiolite is extremely well preserved and the different massifs it is made of are so structurally coherent that along-strike paleo-ridge systems have been mapped out over 100's of kms, and across-strike detailed dating of sheeted dyke complexes allowed for detailed restoration of spreading rates. The obduction-related deformation of the Oman ophiolite led to minor folding and occasional thrusting, but not even a single major repetition of the ophiolite is found, let alone the massive wrench zone the reviewer would need to come with a plausible alternative. Our interpretations are fully consistent with the structure – regional and detailed – of the Oman ophiolite. And even if there would be local rotations, those would by no means affect the paleospreading directions that we reconstruct – the main strength of the net tectonic rotation analysis. As a result, the revisions necessary to fully account for the third reviewer's comments are relatively minor.

The first and second reviewer barely address the contents, but mainly focus on the major implications that our data and kinematic restoration have for the dynamics of subduction initiation in general, and in the Tethys in particular. Their reviews illustrate the high impact of our work. But instead of welcoming the new data, that for the first time actually constrain the initial conditions that pertained to Oman subduction initiation, they reject the data in favor of their dynamic models and require us to demonstrate through dynamic modeling that the data can be correct.
This is philosophically flawed. Data can falsify models. Models cannot falsify data. Both reviews are highly passive aggressive in the sense that they provide no alternative interpretation of our data, and simply discard the evidence. Of course we have

interpretations of the dynamics of this system – in fact, we are preparing papers in which we will offer our interpretations of the dynamic drivers of E-W subduction initiation in the Neotethys – but including those in the current paper would be a disservice to the paper, and to the audience. In the philosophy of incremental science, here we present robust data that is highly relevant at the regional scale, but that is also challenging paradigms in generic subduction initiation. This is a first brick that needs to be laid clean and clear, so that the whole community is free to build on it and this is the purpose of the current paper.
We have now added a final paragraph to the paper in which we explicitly address some key questions for future dynamic analyses raised by the reviewers.
The few remarks on the kinematics of both reviewers – on Turkey, or on the Permian spreading of the Neotethys – come out of thin air and are simply incorrect or entirely unconstrained.

We were pleased to see that you have not taken their arguments into account in your decision to reject our paper. In the rebuttal below we will briefly respond to all requests, and attempted to address as many of the relevant ones as possible into an upgrade of our paper.

We hope you will find this revised version of our paper acceptable for publication in EPSL.

With best regards,

Douwe
Marco
Louise
Carl

Dear Dr. Douwe J.J. van Hinsbergen,

I finally received comments from three reviewers. Two of the referees recommend rejection and one suggests major revision. As you can see from their comments, they feel that (1) the interpretation of the newly obtained paleomagnetic data does not consider the alternative solution/interpretations, (2) a lack of integrating paleomagnetic data with other geologic constraints particularly those already documented in the literature and those at the sampling sites, and (3) the tectonic model is too crude to account what is already known about the region. Although your work may have the potential to make a great impact on the evolution of the Neo-Tethys, it appears that addressing all the concerns will either require the work to be sent to a specialty journal or a complete face-lift in its organization and data integration. Based on this judgement, I recommend that you either send the work to other journal to revise the work completely according to the referees' comments and send back to EPSL as a new paper. I will ask at least one of the original reviewers to assess your new paper and mostly will also involve new referees. If you do decide to resubmit a new manuscript, please make a detailed list of your response to the reviewers' comments. For your guidance, I append the reviewers' comments below. Thank you for giving us the opportunity to consider your work.

Yours sincerely,

An Yin, PhD
Editor
Earth and Planetary Science Letters

Reviewers' comments:

Reviewer #1: Review of the manuscript "Kinematic and paleomagnetic restoration of the Semail Ophiolite (Oman) reveals subduction initiation along an ancient Neotethyan fracture zone", van Hinsbergen et al.

This is a detailed and informative paper, which aims to kinematically restore the orientation of the Oman SSZ spreading ridge during subduction zone infancy. Authors present the first paleomagnetic dataset from the sheeted dykes sections of the Oman ophiolite.

Since I am not a specialist of paleomagnetism, I cannot provide any judgement on the quality of this novel dataset. However, the dataset is precisely described in the text and consistent with the literature, and the figures are very useful. I have therefore based my review on the paleogeodynamic interpretations made by the authors, which I think are the main purpose of the submission of the manuscript in EPSL.

> We make no geodynamic interpretation in our paper. We only constrain the orientation and location of the trench at the moment of inception of subduction. Then based on this, we infer from regional kinematic context that this subduction zone was parallel to fracture zones, including the one along the Oman margin, and our interpretation only concerns the likely structure along which subduction

initiated. We have addressed most comments of the reviewer below by adding a last paragraph to the discussion section:

"Our results, and those of Maffione et al. (2017) for the Mediterranean region, raise several first-order new questions for understanding subduction initiation dynamics. Our results show that Cretaceous subduction initiation within the Neotethys ocean formed a new plate (the Anadolu plate of Gürer et al. (2016) separated from Eurasia and Africa-Arabia by trenches (Figure 8). This plate must have moved westward relative to Africa/Arabia (and Eurasia, given overall N-S Africa-Eurasia convergence) to drive subduction initiation along N-S striking trenches. Gaina et al. (2015) showed based on Indian Ocean reconstructions that prior to the end of the Cretaceous superchron, India rotated counterclockwise relative to Arabia that requires such convergence. Did the driver of this rotation also spark subduction initiation farther westwards? And what processes cause the hot conditions recorded in the Oman metamorphic sole 8 Myr of upper plate spreading (Guilmette et al., 2018) with subduction initiating in old, cold lithosphere? We refrain from speculating on these questions, but leave these for future study and debate."

The authors easily convince the reader that the Semail ridge was oriented N(NE)-S(SW) and therefore the subduction zone nucleated along the same orientation. As mentioned by the authors, this orientation is orthogonal to that of the NeoTethyan mid-ocean ridge, which was anyway likely subducted below Eurasia at the time of the Oman subduction initiation. The model presented by the authors of an intra-oceanic subduction initiation taking place along a fracture zone is very interesting and deserve to be published as it is consistent with their dataset. However, this model does not integrate sufficient constraints to be published in EPSL. That is why I recommend major revision before publication or rejection.

The reviewer does not list any constraints below, only models.

In the authors' model, the subduction zone nucleates along a fracture zone which has an orientation roughly parallel to the general convergence between Eurasia and Arabia, and completely orthogonal to the Zagros subduction. This subduction initiation dynamics is therefore not straightforward to understand and the authors do not propose sufficient details about the potential mechanisms driving this subduction and the associated ophiolite accretion.

The orientation of the initial trench is constrained by observations and measurements and does not require an understanding of what would drive this subduction initiation.

The authors briefly mention a potential E-W contraction as the driver of the subduction

initiation. E-W contraction is possible but a priori quite odd in the NeoTethys Ocean. This point needs to be further argued.

> As we now mention and cite in the manuscript, it has been shown based on magnetic anomalies that the late Cretaceous break-up of India from Madagascar is associated with a counterclockwise rotation of India relative to Africa/Arabia about a pole in the NW Indian Ocean. This rotation demonstrates that there must have been E-W convergence in the Neotethys at this time (Gaina et al 2015). This has been known for well over a decade, and assuming the convergence in the Neotethys was only N-S is inconsistent with the facts. We have added this question to the final part of the discussion.

Moreover, the authors consider that the N-S striking fracture zone was a significant weakness zone within the NeoTethys ocean and may have localized subduction initiation. This fracture zone is located by the authors within a ~170 My old oceanic lithosphere which was therefore mechanically very strong (i.e., large effective elastic thickness).

> The reasoning of the reviewer here is based on the current preferences in the modeling community, while our conclusions are based on unequivocal data, and these data strongly suggest that a new subduction zone formed within a ~170 Ma old lithosphere. Unless the reviewer finds flaws in our data, or has reasons to assume there was an active ridge in the Cretaceous within a Permian passive margin and adjacent ocean basin of which sediments are preserved below the ophiolite, then this conclusion remains. See new final paragraph of the discussion.

The tectonic stress must have been really large to overcome the resistance of a very old oceanic lithosphere, in several places (not only triggering the Oman ophiolite obduction but also that in the westernmost belt) and along not-preferentially oriented fracture zones. In absence of more details on this contraction event (i.e., considering the regional dynamics), the E-W contraction and the position of a N-S striking fracture zone are too speculative.

> We have to disagree. As now explicitly mentioned in the paper, data from the Indian Ocean case (Gaina et al., 2015) unequivocally demonstrate that E-W convergence must have occurred somewhere in the Neotethys north (and west) of India. The latter has previously been identified in Afghanistan and Pakistan, and we show further evidence here. Dynamics are interesting, but we need no understanding of the dynamics driving the system to demonstrate that the system existed, and in which orientation. See new last paragraph of the discussion.

The authors suggest that the arabian margin might have been associated with hyperextension as observed in Guinée (Guillard et al., 2017) that could have facilitated the rupture. However, the Guinean margin is associated with the opening of the Atlantic ocean, and therefore corresponds to a complete different setting. It is very likely that the NeoTethys opening was associated with a higher magmatic activity, making very unlikely the presence of hyperextension margins. Moreover, such hyperextension would essentially

affects the continental lithosphere and not the intra-oceanic lithosphere located along the fracture zone (at several hundred km of the margin).

> The points raised here by the reviewer are quite debatable. First, to our knowledge there are no data indicating the style and intensity of the magmatic activity during the opening of the Neotethys in the Permian. If such data existed, we exhort the reviewer to cite the relevant papers and will take them into account. In the absence of such data, our suggestion remains a logical possibility that fits well with our data. Second, our last Figure, as well as the text, quite explicitly indicates that because old oceanic lithosphere is so stiff, we presume that subduction actually started around the ocean-continent transition, not in the middle of the ocean. That is, admittedly, a suggestion that any reader is free to agree or disagree with. Our data constrain an initial orientation, a paleolatitude, and combined with previous data in Morris et al. (2016), a rotation. Our reconstruction is consistent with our suggestion, but we do not exclude that other alternatives are also possible if the reviewer, or any reader, would provide one. See new last paragraph of the discussion.

While the authors state in the introduction that the thermal conditions of the metamorphic sole formation require an extremely warm environment during subduction initiation, the proposed model is not consistent with such constraint. The onset of the subduction takes place in a very old oceanic lithosphere too cold to provide the heat required to form the metamorphic sole.

> Again, this is philosophically flawed. We demonstrate an initial NE-SW dyke and trench orientation in a Permian ocean, and the temperature of the sole below the Oman ophiolite is demonstrably high. So, our data suggest that to explain the records of ophiolites, a reason has to be found for high temperatures, not discard this evidence because we're not clever enough to come up with a solution. But our data are not requiring providing such a solution at this stage, since it will not change the orientation or location of the subduction zone, nor the angular relationship with the Arabian passive margin. We have added this problem to the list of implications of the paper, but we will not offer a solution, for our data and interpretation do not require one. We believe our paper will stimulate more research in many fields, a hallmark of impactfull papers. This includes research on metamorphic soles

Moreover, it means that the metamorphic sole at 105 Ma was metamorphosed and accreted to an oceanic lithosphere formed at 170 Ma ago. Nowadays, the metamorphic sole is found welded below the Oman ophiolite (96 Ma old). How is this mechanically and structurally possible?

> First, these comments do not address the orientation of the initial trench or the age of the Neotethys ocean, and are thus very interesting, but not relevant for this paper. The answer to this problem, moreover, was explained extensively in van Hinsbergen et al G-Cubed 2015 and Guilmette et al., 2018. the sole is welded to mantle. The crust of an ophiolite is generated in a given time interval, and that of Oman was formed at 96 Ma. The mantle is the mantle. We might be able to date

chemical modifications, but physically it's been mantle for over 4 Ga. Accretion of the sole predates extension in the upper plate and formation of the ophiolitic crust (Guilmette et al. 2018).

Another issue is the accommodation of the slab roll back in the upper plate (future ophiolite). Since the rotation of the ophiolite postdates its magmatic accretion, the whole ophiolite (and the metamorphic sole already accreted) must have undergone significant tectonic extension and this must have happened in a relatively cold environment. Is there any field evidence to support this hypothesis?

We do not understand why extension must have happened in a cold environment, nor what this actually means. The Oman ophiolite preserves a 50 km wide strip of ocean floor formed until 95.5 Ma. This doesn't imply that this was the only SSZ crust formed at that time. All oceanic crust that formed after this time must be located to the north and east of the ophiolite, offshore Oman. During SSZ spreading orthogonal to a trench, the ridge in the upper plate migrates away from the trench at half spreading rate. The narrow age range of ophiolites does not show that spreading was short lived. Ophiolites simply only preserve a narrow strip of the original upper plate, as we already explained in the paper. So magmatic accretion may have continued for tens of Myr to facilitate roll-back, and the environment at that back-arc ridge may have been very hot – which we had already explained in the original paper.

Moreover, I imagine that the roll back is partly accommodated by a large transform fault on the eastern flank of the subduction zone. Is there any evidence for such a structure in the gulf of Oman?

We agree with the reviewer: there must have been a large transform fault accommodating the roll-back and clockwise rotation of the ophiolite, which is indicated in Figure 8. The plate boundary between the Arabian plate and India is a transform, currently represented by the Owen fracture zone. This boundary has a long and dynamic history, and post-90 Ma motion has undoubtedly obliterated the original boundary. But the crust to the west of this boundary in the Gulf of Oman is of normal polarity with no reversals, consistent with formation during the Cretaceous normal superchron as in our reconstruction.

I have also some concerns with the drawing presented in figure 8.
Figure 8b: What is the significance of the dash line? Is it a transform fault linking two fracture zones? Was such a structure already reported?

No, it is located in lithosphere now lost to subduction and collision in the Zagros, so this structure was not reported. But there is a N-S trending trench in eastern Anatolia, and one in Oman, and simple plate kinematics requires a transform fault in

between. Not drawing it violates the basic rules of plate tectonics. We explained in the figure caption:
"Basic plate kinematics requires that the N-S subduction segments were connected with a transform fault parallel to (and here dotted along) the Arabian passive margin."

Figure 8d: the ridge axis is drawn offshore, while it should be inland (i.e., obducted). What happened to the large oceanic lithosphere between the ridge and the trench? This area is much larger than that of the present-day obducted ophiolite.

Yes, of course the area is much larger than the obducted ophiolite. There is no reason whatsoever to assume that Cretaceous spreading stopped where the modern ophiolite reaches a late Holocene coast. Rioux et al shows that we have only one half of a spreading record in Oman, one with a coast-ward younging dyke complex. Previous interpretations have suggested that there may be symmetric, short-lived ridge systems within the ophiolite that jumped, but we see no reason to assume that the spreading of the crust ceased after 50 km of ultra-fast spreading. There is at least 100 km of obducted ophiolite on Arabia's passive margin offshore northern Oman, and lithosphere without magnetic anomalies, consistent with formation in the Cretaceous superchron as in our model, all the way to the trench of the Makran, so there is no reason to discard our scenario with spreading until Maastrichtian obduction. This point was already explicitly discussed in the paper.

Reviewer #2: I have read this manuscript carefully several times over in order to understand the inferences made by the authors based on their palaeomagnetic data from the sheeted dykes and lava sequences in the Oman ophiolite and their model of subuction initiation and SSZ formation / emplacement of this ophiolite. The manuscript has two main parts: the first part involves the presentation of new palaeomagnetic data from the sheeted dykes and lavas in the Oman ophiolite. The palaeomagntic data and the related discussions follow the scientifically established methods, although there are hardly any structural observations and data from the sheeted dykes and the extrusive sequence in the ophiolite that may explain some of the reported rotational deformation (no horizontal rotation due to intra-oceanic faulting?).

The net tectonic rotation analysis (Allerton and Vine, 1987) used in this study requires two input data: (i) the *in-situ* site mean remanence direction, and (ii) the current strike and dip of the dykes. We obtained both these data and no further structural constraints are required to compute the net rotation at each sampling site. The net tectonic rotation analysis calculates the net rotation (no matter how many phases of rotation occurred and along which axis) about an inclined axis. This means that when the returned rotation axis is shallow the tilt component is

predominant over the vertical-axis rotation component and vice versa. Since our data show rotation axes that are not vertical but steeply dipping, this implies that some tilt must have occurred during the deformation history (as observed at the two pillow lava sites MA01 and MA02). This can either be related to intra-oceanic faulting or to any other recent faulting, it doesn't really matter. That being said, the other result of the net tectonic rotation analysis is the initial strike of the dyke. This is totally independent on the number and kinematics of rotational phases. So, no matter what the deformation was, the initial dyke orientation will always be the same, and this is the main constraint that we use in this study to determine the geometry of the subduction zone in the Neotethys. Finally, regional vertical axis rotation of the entire ophiolite has extensively been documented by Morris et al. 2016, and the regional coherence of the ophiolite have been demonstrated for decades by Adolphe Nicolas and many others. So we do not understand what additional structural observations we should have taken into account that the reviewer considers as relevant?

The second part deals with where and how the Neotethyan subduction that was responsible for the SSZ evolution of the Oman ophiolite might have started. This second part, which the authors claim as the main purpose of this paper, presents some problems, which I explain below.

(1) The authors state that the subduction within the Neotethyan realm started along a continental margin parallel fracture zone, and the Oman ophiolite evolved above this subduction zone as a SSZ oceanic lithosphere. The eastern margin of the Arabian continent was then in the upper plate of this subduction zone for nearly 10-15 million years. However, there is no record of subduction-related Cenomanian magmatism on the Arabian plate that would have been expected from such an Andean-type continental margin evolution. A weak point in the model.

There is indeed no record of upper plate magmatism on Arabia, but this may be straightforwardly explained. The reviewer does not consider that upper plate magmatism only starts when the slab has reached some depth sufficient to trigger melting. Numerical models suggest some ~100-150 km or so. At the same time, upper plate extension and ophiolite spreading started when the slab became long enough to exert slab pull. Numerical modeling previously suggested that this happens when a slab reaches 100 km length (e.g. Leng & Gurnis). Between 105 and 95 Ma, convergence may well have been (and probably was) very slow and therefore roll-back started before the slab was able to generate the magmatic arc. Once that depth was reached, magmatism was accommodated close to the trench forming an SSZ ophiolite.

(2) The authors propose, based on their palaeomagnetic data, a nearly 150° CW rotation of this subduction zone and the seafloor spreading system above the slab in order to explain the SW emplacement of the Oman ophiolite in the latest Cretaceous. Yet, there is no explanation in the entire model as to what caused this significant rotation of the subduction - seafloor spreading system. I cannot see any geodynamic forcing in the model figure (Fig

8b) that would even hint a reasonable mechanism for such a large-magnitude rotation in intra-oceanic conditions. Another major weakness in the model.

The rotation follows from a very large number of paleomagnetic studies (see Morris et al., 2016 for a comprehensive review) and is widely accepted amongst the scientific community. Not providing a dynamic explanation for such rotation is not a weakness to constrain the original orientation and position of the subduction zone – in fact, it's completely irrelevant.
The mechanisms to produce even larger intra-oceanic rotations (~200°) have been discussed for example by Chertova et al., JGR 2014. The answer is probably the interaction of the southern (now northern) tip of the trench with the Oman margin. This is intra-oceanic rotations occur almost everywhere – Banda, Northern Caribbean, Gibraltar, Cyprus. So, this mechanism is actually quite simple and irrelevant to our conclusions.

We added to the discussion, where we calculate the long-term roll-back rate: "*This gives an average long-term drift rate of ~4 cm/yr, which is well within the ranges of similar strongly rotating trenches that roll back along and obduct passive margins (e.g., Chertova et al., 2014).*"

(3) The tectonic model presented in Figure 8 is highly crude in terms of the shapes, geometries and regional extents of the continental and oceanic domains. This is a problem because the model then becomes a whimsical cartoon, which falls apart when we look at the Cretaceous palaeogeography of the Neotethyan oceanic realm and the surrounding continents. I presume that the eastern extension of the Greater Adria in Figure 8B is the Tauride-Armenian Platform, although it is not labelled appropriately. But, the sharp termination of this platform (?) by a NNE-SSW - oriented fracture zone on the east is fictional, and there is no geological evidence for its existence in the past. In reality, this platform extended all the way to the NE, near the Eurasian margin longitudes, as we can now observe in the South Armenian Platform.

We have added labeling of Greater Adria. We show the Tauride platform (and the Bey Daglari foreland in the west), and the Kirsehir-Tavsanli blocks. This is a simplified, but accurate reconstruction of eastern Mediterranean paleotectonic map, based on the most detailed tectonic (GPlates) restoration of the Mediterranean region that exists to date (van Hinsbergen et al., Gondwana Research, invited paper in prep). Contrary to popular view in the literature on the South Armenian Block, this block was not part of the Tauride platform, but was separated from it by an oceanic branch that emplaced Cretaceous ophiolites southward onto the Taurides even before the South Armenian block became obducted by Eurasian margin (Jurassic) ophiolites. South Armenia is included in the reconstruction, but lies off the maps of the figure, to the north.
But in any case, the NNE-SSW fracture zone is unequivocally demonstrated by the South Armenian block and easternmost Taurides, which disappear abruptly eastwards, where they give way to the much older Iranian Cimmerides. Moreover, the orientation of the subduction system in eastern Anatolia also followed from

paleomagnetic constraints from sheeted dykes from a large number of eastern Mediterranean ophiolites (Maffione et al., 2017). The detailed paleogeography of the Mediterranean region is beyond the scope of our paper, and the reader can find the details in Maffione et al 2017.

(4) The purported E(SE) - W(NW) - directed contraction within the Neotethyan realm that led to subduction initiation, followed by ophiolite emplacement, has no valid explanation from the point of the regional geodynamics. What caused this inferred E-W contraction within Neotethys? There is no explanation in the manuscript for the cause of this major contractional episode. Yet, there are plenty well-documented and explained models in support of a SSW to NNE directed contraction in this region (nearly 90° different from the authors' proposed direction) that was induced by the relatively fast motion of Afro-Arabia in the same direction, caused by the opening of the South Atlantic Ocean during the Cretaceous (see all the reconstructions by A.G. Smith et al., etc.). The authors should have at least discussed some of these previously published models and explanations for the direction(s) and mechanisms of the closure of Neotethys.

Nowhere in our paper do we contest that the convergence direction between Arabia/Africa and Eurasia was N-S. We show in our reconstruction that this convergence was accommodated at a well-documented trench along the Eurasian margin, from the Pontides to Tibet. So we don't need to address the reconstructions of Smith, or anybody else, because they're fine where it comes to the convergence direction between Arabia and Eurasia. But the plate that formed by initiating subduction within the Neotethys around 105 Myr was not Eurasia, and not Arabia, and the motion of this plate was unconstrained in previous models, but simply assumed to partition Africa-Eurasia convergence, of any kinematics were ascribed to it in the first place. Our analysis strongly suggests that this 'Anadolu plate' as defined by Gürer et al. (2016) moved westward, at least for the short duration of subduction initiation, relative to both. This does not violate any of the Atlantic models – in fact, those models are incorporated in the reconstructions of Figure 8.
To make this explicit, we have added this to the final paragraph of the discussion.

(5) Large-magnitude CW or CCW post-magmatic rotations (90° and more) have not been reported from the Cretaceous ophiolites exposed in Southern Turkey, particularly from the north and south of the Tauride carbonate platform, and thus the ophiolite emplacement mechanisms depicted in Figure 8D do not work.

These rotations have actually been documented recently by Maffione et al., JGR 2017 and Morris et al EPSL 2017, and previously by Inwood et al., 2009 EPSL for ophiolites that were emplaced both northward and southward onto the Taurides. In particular, the ophiolites of Troodos (Cyprus) and Hatay and Baer-Bassit in Syria underwent a widely documented ~90° of intra-oceanic rotation, according to a mechanism similar to that we have proposed in this study and that is fully consistent with our reconstruction.

Reviewer #3: Based on a palaeomagnetic investigation of sheeted dykes from the Oman ophiolites, the authors determined the net rotation history of 7 out of 10 sampled ophiolite sections from which they restored the dykes' original orientations using the method of Allerton & Vine (1987). According to authors' preferred solution, the original subduction zone is inferred to dip WNW. Based on this interpretation they argue that the subduction was likely initiated along an ancient, continental margin-parallel transform-fault fracture zone, induced by (WN)W-(ES)E contraction. From a paleomagnetism perspective, I feel that the most critical assumption of the manuscript is that the authors accepted only the first net tectonic rotation solution but refused an alternative rotation solution; the latter requires an WNW strike of the original subduction zone induced by non-uniform tectonic rotation pattern involving both CW and CCW rotations at different dyke sampling sections. Considering the direction of the original subduction zone of the alternative solution is almost perpendicular to the preferred solution by the authors (the alternative solution yields a near N-S spreading and approximately parallels to the Arabian passive-margin/the Neotethyan ridge), clear evidence from field and in particular structural observations is essential. That is, the authors need to show whether the sampled dyke sections in Oman experienced similar tectonic rotation patterns around near-vertical axes rather than different rotation patterns during the obduction. In short, the authors must incorporate the non-uniqueness of the paleomag data interpretations in the discussion.

> First, the reviewer asks for vertical axis rotation confirmation of the clockwise rotation scenarios. Such evidence is extensively provided from both effusive rocks, and gabbros, by Morris et al., 2016 (see in particular our Supplementary Figure 2, which summarizes the pmag data (tilt corrected) from all sites in Oman having a paleo-horizontal control. This dataset clearly indicates an overall large CW rotation of the whole ophiolite, with minor local rotations that produce the observed scatter between ~70°CW and ~160°CW around an average of ~120°CW. So, based on this, counterclockwise solutions can certainly been discarded. The only difference in rotations are in the southernmost part of the ophiolite, which, according to Morris et al. (2016) and Feinberg et al (1999), has been remagnetized during the late Cretaceous obduction. The rotations in the rest of the ophiolite are consistently CW and above ~100°. This already excludes the reviewer's perceived alternative.
>
> Demanding vertical axis rotation constrains from sheeted dyke sections is impossible because these units do not yield a paleo-horizontal control and a classical "tilt correction" of vertical units has been demonstrated to lead to incorrect rotations. If that would have been possible, we wouldn't have bothered to perform a net tectonic rotation analysis in the first place.
>
> Finally, regarding the non-uniqueness of the paleomagnetic data, we have now added additional explanation on the criteria used to select a preferred solution out of the two alternative solutions (see Methods). The main reason for rejecting one of the two solutions (note in the table we have sorted the preferred solution in the first column and the alternate in the second column, so the preferred solution wasn't

always the first solution of our net tectonic rotation analysis) is that the rejected solutions require either (i) a rotation kinematics that is not consistent with the regional pattern (e.g., CCW rotations are not possible considering the regional CW rotation of the ophiolite), or (ii) a restored orientation of the various units after back-rotation that is inconsistent with the mapped structure – many require that the ophiolite is overturned where it clearly isn't, or strikes of unit boundaries that are far off the modern strikes. These constraints show that what we have selected as "alternative solutions" is clearly not permitted.

Minor comments:
Lines 247-251: interpretations of the existence of sulphides in these sites need more work. If the sulphides have contributed to magnetic susceptibility up to more than 50% of the sample, why does the cooling curve show much lower magnetic susceptibility when breaking down to the strong ferromagnetic magnetite above ~500 Celsius degrees?

Possible occurrence of iron sulphides have only been suggested for sites DA and HA based on the gentle inflections of susceptibility observed in the heating curves of thermomagnetic experiments. This is, therefore, not a common feature observed everywhere within the study area and we don't understand what kind of "more work" should be done on the existence of iron sulphides. Beside this, we have not stated anywhere in the paper that "*sulphides have contributed to magnetic susceptibility up to more than 50% of the sample*", so we don't understand really what the problem is here.
Regarding the evidence that the cooling curve of susceptibility has lower values than the heating one this is simply because any reaction induced by heating in our experiments has not produced new magnetite because the experiments were carried out in argon atmosphere, hence in reducing conditions. So, the breakdown of ferromagnetic iron sulphides have just removed this phase from the system without generating new magnetite (hence the lower susceptibility). We have now incorporated this explanation in the main text.

Line 251-252: severely distorted description shown in the plot. the susceptibility seems not to drop to zero at temperatures as high as ~700 C.

We don't understand why our description is distorted. We used the standard method of Petrovsky et al. (2006) to determine the Curie temperature at site AS using the thermal variation of magnetic susceptibility shown in Figure 2, and we obtained a value of 595°C. This value is higher than the Curie temperature of pure magnetite (which is 580°C) and more similar to that of maghemite (see Dunlop and Ozdemir, 1997). What is wrong with this?
Regarding the second point, we do not know why susceptibility does not drop to zero (it gets really close to zero though). It must have something to do with the calibration of the instrument. However, in this kind of experiment the absolute

values are completely trivial as only the shape of the curve is used to infer the Curie temperatures of the ferromagnetic minerals.

Lines 258-260: Due to problematic descriptions/interpretations of the data mentioned above, this paragraph and particularly this summary needs to be rewritten.

Again, we don't understand why our description is distorted. For each site described in this section we applied the standard method of Petrovsky to determine the Curie temperatures and based on this, the occurrence of titanomagnetite at e.g. sites MA01 is unequivocal. These Curie temperatures are further supported by the thermal demagnetization experiments, as we already state in the main text. We have slightly reworded this paragraph to make it perhaps a bit clearer, but the values and our interpretation is correct and has not been modified.

Lines 261-266: this part needs supporting references and/or additional analyses to reinforce the interpretations.

Thanks for the suggestion, indeed this was missing. The link between the shape of the hysteresis loops and the grain size is discussed in the book Dunlop and Özdemir (1997), which has now been cited in this paragraph.

lines 281-284: need supporting references.

We have deleted this sentence as it was redundant based on what we state in the previous sentence.

Lines 303-305: What about the remanence borne by the maghemite? Is there any evidence from the SEM observation for the representative samples that provide constraints on this maghemization?

No, we don't have clear evidence for the occurrence of maghemite based on the thin section observations. We have now stated this in this section. However, maghemitization may only affect a thin portion of the outer rim of magnetite, forming a thin coating of maghemite, which is difficult to identify at the SEM (cracks are typically the evidence suggesting the occurrence of maghemite).

Lines 326-336: Due to the difficulty in interpreting the abnormal directions and even the reversed directions from site BB, the authors excluded this observation from further analysis. Given that you have done some rock magnetic experiments and SEM observations for the representative samples from each sampling site, do you have any robust evidence to support this action? In other words, I have a great difficulty to see the difference in rock magnetism and SEM observations within the significantly remagnetized sites (AA and MU),

and possibly remagnetized site BB, and all the accepted sites.

> We thank the reviewer for raising this important point. We have now adopted a different approach to discuss the potential remagnetization of those sites, and have substantially rewritten this part. First, we have now initially considered the remanence from sites BB, AA, and MU, and have used them for the net tectonic rotation analysis. Then, we have discussed the results from the net tectonic rotation analysis for these site, and have concluded based on this additional evidence that sites BB and MU must have been remagnetized. Site AA gave actually quite reliable results and an initial dyke orientation consistent with the other sites (i.e., ~N-S). However, as discussed now in the main text, we have decided to discard this site from further discussion as the potential for error associated to the rotation parameters is very high.

Lines 344-348: Inconsistent statement and self-contradictory conclusion. According to the discussion of the palaeomagnetic data (lines 315-336), three (i.e. AA, MU, and BB) out of 9 sites were interpreted as being remagnetized, why are they concluded as primary records? On the other hand, according to this discussion, the site HA, which has a A95 significantly less than the A95min (Table 1), might fail to effectively average out the PSV. Hence, it should have precluded a significant tectonic rotation. However, this is not discussed.

> We have now significantly expanded this discussion and partially rewritten this section. All points raised by the reviewer here have been addressed and clarified.

Lines 357-361: This is the most important part of the manuscript. Due to the very complicated deformation history during the obduction of the ophiolite carrying sheeted dykes, serious and very possibly heterogeneous deformations associated with vertical-axis rotation might have occurred at the sampled dyke sections. The authors' preferred solution was based upon the hypothesis that the sheeted dykes experienced only large near-vertical clockwise rotations during the deformation. This might be the case according to previous palaeomagnetic studies. However, field observations at each sampling site is needed to support this interpetation. Otherwise, the authors should at least mention and discuss this alternate possibility.

> The reviewer's comment '*Due to the very complicated deformation history during the obduction of the ophiolite carrying sheeted dykes, serious and very possibly heterogeneous deformations associated with vertical-axis rotation might have occurred at the sampled dyke sections*' is entirely unsupported by evidence. This is, in fact, a complete speculation. Of course there is some local deformation in the ophiolite, particularly extensional related to the original spreading, and there are large, open folds and an occasional thrust. But there is nothing 'very complicated'. Nowhere are regionally important duplications within the ophiolite reported, there are no tens of km wide completely chaotic strike-slip faults or former fracture zones, etc etc. In fact, the ophiolite is so extremely coherent that for decades people have mapped out complex ridge systems and spreading rates. The regional clockwise

rotation was extensively documented by Morris et al and is consistent with our findings, and that of others. So our choice of the preferred solutions based on the expected rotation pattern (i.e. large CW vertical-axis rotations) is quite solid and reliable. We have now clarified the three criteria adopted for the choice of the preferred net tectonic rotation solutions. It is now possible to note that the regional CW vertical axis rotation is not the only criterion used to select our preferred solutions. Furthermore, we have now expanded the discussion of the preferred and alternate net tectonic rotation solutions, and have clarified better how and why we selected those particular solutions as preferred. So, in conclusion, the claim of the reviewer that everything is chaotic is incorrect and fails to explain the structural and paleomagnetic coherence.

Figure 6: please indicate the meanings of different symbols/lines in the diagram. As many great circles are used in the calculation of the ChRMs, adding a few representative orthogonal and stereographic plots may help clarify the demagnetization trajectories.

We have now added additional explanations of the symbols in the relative figure caption. Representative Zijderveld plots have already been presented in Figure 5 and Figure 6 is already too large to add more Zijderveld plots there.

Table 1: Please correct the clerical mistakes or inconsistent numbers in the "ChRM interpr." and "n/N" columns, such as those for site DA, MA01, and MA01/02.

We have corrected the numbers for site DA, although those of sites Ma01 and MA02 are correct, as the n/N values are different for in situ and tilt corrected data.

Table 2: Please following the work of Allerton & Vine (1987) and use the "Rotation vector" rather than "Rotation axis".

Although both terms are correct, we prefer the term “rotation axis” as it will be more clear to a non specialized reader.

Kinematic and paleomagnetic restoration of the Semail Ophiolite (Oman) reveals subduction initiation along an ancient Neotethyan fracture zone

Douwe J.J. van Hinsbergen[1], Marco Maffione[1,2], Louise M.T. Koornneef[1,3], Carl Guilmette[4]

1. Department of Earth Sciences, Utrecht University, Heidelberglaan 2, 3584 CS Utrecht, Netherlands
2. School of Geography, Earth and Environmental Sciences, University of Birmingham, B15 2TT, UK
3. School of Geography, Earth and Environmental Sciences, Plymouth University, Drake Circus, PL4 8AA Plymouth, UK
4. Département de Géologie et de Génie Géologique, Université Laval, Québec, QC G1K 7P4, Canada

For: EPSL

Abstract

The archetypal Semail ophiolite of Oman has inspired much thought on the dynamics of initiation of intra-oceanic subduction zones. Current models invoke subduction initiation at a mid-oceanic ridge located sufficiently close to the Arabian passive margin to allow initiation of continental subduction below the ophiolite within ~10-15 Myr after the 96-95 Ma age of formation of supra-subduction zone crust. Here, we perform an extensive paleomagnetic analysis of sheeted dyke sections across the Semail ophiolite to restore the orientation of the supra-subduction zone ridge during spreading. Our results consistently indicate that the ridge was oriented NNE-SSW, and we infer that the associated trench, close to the modern obduction front, had the same orientation. Our data are consistent with a previously documented ~150° clockwise rotation of the ophiolite, and we reconstruct that the original subduction zone was WNW-ward dipping and NNE-SSW striking. Initial subduction likely occurred in the ocean adjacent and parallel to the Arabian transform margin that formed the original underpinnings of rocks in the Zagros fold-thrust belt, now underthrust below Iran. Subduction thus likely initiated along an ancient, continental margin-parallel fracture zone, as also recently inferred from near-coeval ophiolites from the eastern Mediterranean and NW Arabian regions. Subduction initiation was therefore likely induced by (WN)W-(ES)E contraction, and this constraint may help the future identification of the dynamic triggers of Neotethyan subduction initiation in the Late Cretaceous.

1. Introduction

Subduction initiation is a critical step in the plate tectonic cycle, and how and where subduction zones form has therefore been at the forefront of geodynamic research for decades (e.g., Guilmette et al., 2018; Hall et al., 2003; Stern and Gerya, 2017). Ophiolites, i.e. exposed fragments of oceanic lithosphere that are often found thrust upon continental margins, have played a central role in the development of concepts of subduction initiation (Pearce et al., 1984; Stern et al., 2012). First, Pearce et al. (1984), among others, recognized that most ophiolites contain geochemical evidence that indicate formation at a spreading center located above a subduction zone (for this reason called supra-subduction zone (SSZ) ophiolites). Second, many SSZ ophiolites are associated with metamorphic soles - typically high-temperature, low to high-pressure metabasalts and metasediments that are found below the ophiolite's mantle section, thought to have been derived from the top of now-subducted oceanic lithosphere. Their high metamorphic temperatures are atypical for mature, cool subduction zones and metamorphic soles are therefore thought to form at the plate contact during subduction zone infancy (e.g., Agard et al., 2016; Boudier et al., 1988; Guilmette et al., 2018; Hacker and Gnos, 1997; Pourteau et al., 2018; Soret et al., 2017; van Hinsbergen et al., 2015; Wakabayashi and Dilek, 2003). Because both the upper plate - the ophiolite - as well as the down-going plate in these systems are oceanic, as deduced from oceanic lithologies in the metamorphic soles and underlying subduction mélanges, SSZ ophiolites are thought to result from intra-oceanic subduction initiation (Agard et al., 2007; Stern et al., 2012; van Hinsbergen et al., 2015; Wakabayashi and Dilek, 2003).

Models of intra-oceanic subduction initiation logically point at pre-existing weakness zones within oceanic lithosphere as locations where subduction zones may form, either spontaneously or induced (e.g., Agard et al., 2007 ; Guilmette et al., 2018; Stern et al., 2012), at or near active intra-oceanic plate boundaries: transform faults or young fracture zones, ridges, or ridge-parallel detachment faults (Agard et al., 2007; Boudier et al., 1988; Duretz et al., 2016; Hall et al., 2003; Maffione et al., 2015a; Stern et al., 2012; van Hinsbergen et al., 2015).

Along the northern margin of Arabia, and as the highest structural unit in a microcontinent-derived fold-thrust belt in the eastern Mediterranean region, a discontinuous, ~4000 km-long belt of SSZ ophiolites is found with well-constrained crustal ages of ~96-90 Ma (Maffione et al., 2017; Rioux et al., 2016). The best-exposed and most complete of these is the Semail ophiolite of Oman, and has allowed mapping out 100's of km long, coherent fossil ocean floor (e.g., Nicolas et al., 2000). This ophiolite has inspired much thought on the process of subduction initiation and is widely considered to have formed in the incipient stages of an intra-oceanic subduction zone.

Given the overall N-S long-term Arabia-Eurasia plate convergence, subduction is widely considered to have formed along an ~(WN)W-(ES)E striking mid-ocean ridge within the Neotethys (e.g., Duretz et al., 2016). As drivers for subduction initiation, for instance a far-field driven Arabia-Eurasia convergence rate increase of 2-3 cm/yr (Agard et al., 2007) was proposed. However, paleomagnetic constraints from sediments and igneous rocks of the ophiolite indicate that the Oman ophiolite underwent a major, clockwise vertical axis rotation of as much as

150° (e.g., Perrin et al., 2000; Morris et al., 2016). Back-rotating the present-day obduction front (as a proxy for the intra-oceanic trench location) according to these data suggests that the spreading center at which the Oman crust was formed had a NE-SW orientation, hence almost orthogonal to the Arabian passive-margin, not parallel to it. Second, the earliest metamorphism of Arabian passive continental margin rocks found below the Oman ophiolite is dated at ~80-85 Ma old (Warren et al., 2005), i.e. the Arabian passive margin was already buried at the trench only ~10 Myr after supra-subduction zone ophiolite formation. This suggests that subduction initiated close to the Arabian passive margin, as also indicated by paleomagnetic paleolatitudes (Perrin et al., 2000) and incorporated in various numerical and analogue models (Duretz et al., 2016). Opening of the Neotethys ocean and formation of the Arabian passive margin, however, was Permian in age, and thus occurred as much as ~170 Myr prior to Cretaceous subduction initiation (e.g., Béchennec et al., 1990; Stampfli and Borel, 2002). The presence of a Cretaceous mid-ocean ridge close to a Permian passive margin is unlikely, particularly since the original Neotethyan mid-oceanic ridge must have already subducted below the Eurasian margin in Jurassic time (Maffione et al., 2017; Stampfli and Borel, 2002).

In this paper, we provide the first paleomagnetic dataset from the sheeted dyke sections of the Oman ophiolite to kinematically restore the orientation of its SSZ spreading ridge during subduction zone infancy. To this end, we collected a large paleomagnetic data set from ten localities in sheeted dyke sections along the strike of the Oman ophiolite to determine the net rotation history of the ophiolite and restore the dykes to their original orientation. We then place the Oman ophiolite

in plate kinematic context using the configuration of the Arabian passive margin restored for continental subduction in the Zagros mountains (McQuarrie and van Hinsbergen, 2013), cast in a paleomagnetic frame of reference (Torsvik et al., 2012). Finally, we discuss the implications for the tectonic setting and nature of the weakness zone that facilitated Oman's subduction initiation, and search for settings in today's snapshot of plate tectonic history that may provide an analogue.

2. Geological setting

The Semail ophiolite in Oman consists of a large, well-preserved oceanic lithosphere thrust slice containing a 4-7 km thick crustal sequence, and a 8-12 km thick mantle sequence (e.g., Nicolas et al., 2000). The ophiolitic sequence displays a Penrose pseudostratigraphy composed from top to bottom of a sedimentary cover (radiolarian cherts), volcanics (pillow lavas and lava flows), sheeted dykes, isotropic and layered gabbros, peridotites (harzurgites and dunites), and a 300-500 m thick metamorphic sole with an inverted metamorphic grading (e.g., Cowan et al., 2014; Hacker, 1991; Nicolas et al., 2000; Searle and Cox, 1999; Soret et al., 2017). The ophiolite overlies a sequence of deep-marine, Permian to Cretaceous sediments interpreted to be derived from the distal Arabian margin or the adjacent oceanic crust – the Hawasina nappes – and underlying Arabian margin-derived nappes (Béchennec et al., 1990).

In the northern part of the ophiolite, the extrusive sequence is geochemically layered (Ernewein et al., 1988; Nicolas et al., 2000). Basalts with a geochemistry

similar to mid-ocean ridge basalts (N-MORB) dominate in the lower part of the volcanic sequence, called *Geotimes Unit* or *Unit V1* by Ernewein et al. (1988). Above this unit are the Lasail and Alley volcanic suites, collectively termed *Unit V2* by Ernewein et al. (1988), which consist of depleted arc tholeiites and boninites interpreted as products of hydrous melting of a previously depleted mantle source (e.g., Godard et al., 2006). This geochemical pattern in the crustal sequence of the Oman ophiolite led to the formulation of different tectono-magmatic models invoking formation either in an open ocean (e.g., Nicolas, 1989) or above an active subduction zone (e.g., Pearce et al., 1984). A more recent study, however, suggested that the Geotimes MORBs may have been produced under high water content, hence more likely above an incipient subduction zone (MacLeod et al., 2013).

Paleomagnetic data from the extrusive sequence of the Semail ophiolite indicate a rigid block clockwise (CW) rotation up to ~150° in the northwestern segment of the ophiolite (north of the Hawasina tectonic window), and only minor counterclockwise (CCW) rotations up to ~20° in the southeastern portion of the ophiolite (Feinberg et al., 1999; Perrin et al., 2000; Weiler, 2000). This was originally interpreted as the result of major relative rotations between the northern and southern part of the ophiolite (Nicolas et al., 2000; Perrin et al., 2000), until Feinberg et al. (1999) and Morris et al. (2016) documented the occurrence of a pervasive remagnetization of the ophiolite in the southern segment, which occurred during or soon after the Late Cretaceous emplacement of the ophiolite above the Arabian continental margin (e.g., Nicolas et al., 2000; Searle and Cox, 1999; Searle et

al., 2004). In particular, Morris et al. (2016) suggested that the minor CCW rotation of the southern block occurred after the remagnetization event.

Zircon U-Pb dating of the plutonic section of the Semail ophiolite indicates that the ophiolitic crust formed at a fast spreading ridge in less than ~1 Ma in the Late Cretaceous (~96-95 Ma; Rioux et al., 2016), only just preceding other Neo-Tethyan ophiolites from Turkey and Cyprus with 94-90 Ma ages (e.g., Maffione et al., 2017). Zircon U-Pb and hornblende and mica Ar-Ar ages from garnet-bearing metamorphic sole rocks are similar or slightly younger than the magmatic sequence (96.2-92.6 Ma; Hacker et al., 1996; Rioux et al., 2016; Warren et al., 2005), indicating cooling and exhumation of the sole synchronous with upper plate spreading and formation of the ophiolitic crust (e.g., van Hinsbergen et al., 2015). More recently, garnet Lu-Hf ages from the uppermost, garnet-bearing layer of the metamorphic sole in Oman have constrained subduction-related prograde metamorphism at 104 Ma (Guilmette et al., 2018) and a nearly identical Lu/Hf age was reported from Turkey (Pourteau et al., 2018), indicating near-synchronous timing of subduction initiation. According to these new results, upper plate spreading (and ophiolite formation) postdated the initiation of subduction by ~8-12 Ma. Because spontaneous subduction initiation requires initial slab roll-back and simultaneous upper plate extension (Stern et al., 2012), this delay demonstrates that subduction initiation must have been induced (Guilmette et al., 2018), i.e. triggered by a far-field tectonic stress.

3. Sampling and methods

A total of 380 standard paleomagnetic samples were collected from 12 localities within the sheeted dyke section (10 sites) and the extrusive sequence (2 sites) (Figure 1). All samples were drilled in the field using a water-cooled portable rock drill, and were oriented in situ using both magnetic and sun compasses. Mean paleomagnetic directions for each sampling site were calculated by averaging characteristic remanent magnetizations (ChRMs) interpreted from typically 20-50 samples collected from six to eleven adjacent chilled margin-bearing dykes. Orientation of the volcanic sequence at two sites was determined using the primary layering of pillow lavas and an intercalated lava flow unit.

The nature of the magnetic carriers was characterized through rock magnetic experiments and thin section analysis carried out at the paleomagnetic laboratory 'Fort Hoofddijk' at Utrecht University (Netherlands). High-temperature thermal variation of the magnetic susceptibility was investigated via heating-cooling cycles from room temperature to 700°C in argon atmosphere using a KLY-3 Kappabridge (AGICO) coupled with a CS3 apparatus. The Curie temperatures were determined from the thermal demagnetization results. Hysteresis parameters were calculated through hysteresis loops with peak fields of 0.6-1.5 T, using an alternating gradient magnetometer (Micromag AGM, Princeton). Mineralogical assemblages and the nature and distribution of the ferromagnetic minerals were determined by analizing polished thin sections under both transmitted light and scanning electron microscope (JEOL JCM-6000), and by carrying out elemental analysis with an energy-dispersive X-ray (EDX) analyzer coupled with the SEM.

Remanence components were analyzed using mainly stepwise alternating field (AF) demagnetization with variable increment steps from 5 to 100 mT. About 10% of the samples were also demagnetized thermally in a magnetically shielded furnace (ASC, TD48-SC) using variable increment steps from 100° to 580°C (or until complete demagnetization). AF demagnetization and measurement of the remanence after each demagnetization step were conducted using a robotized superconducting (SQUID) cryogenic magnetometer (Mullender et al., 2016) located in a magnetically shielded room. Demagnetization data were plotted on orthogonal diagrams (Zijderveld, 1967) and the remanence components were isolated via standard principal component analysis (Kirschvink, 1980) using the online software package www.paleomagnetism.org (Koymans et al., 2016). ChRM components with maximum angular deviation (MAD) larger than 10° were discarded from further analysis. Site mean ChRM directions were computed using Fisherian statistics (Fisher, 1953) on virtual geomagnetic poles (VGPs) associated to the isolated ChRMs, and after having applied a fixed 45° cutoff to the VGPs.

The computed site mean directions were then used to calculate the tectonic rotations at each site using a net tectonic rotation approach (Allerton and Vine, 1987). This technique prevents possible biases associated with classic tilt correction in units lacking paleohorizontal constraints, like sheeted dykes, and has been successfully applied to other ophiolites (e.g., Maffione et al., 2017; Morris et al., 1998). Rather than decomposing the deformation into a tilt and a vertical axis rotation component, a net tectonic rotation analysis computes the single rotation around an inclined axis that ~~to~~ restores both the rock unit to its original orientation

(i.e., vertical for sheeted dykes)~~,~~ and the measured *in situ* remanence to a selected reference direction. The reference direction is the direction of the magnetic field at the time and latitude at which the remanence was acquired. ~~The reference direction for this study has been calculated using the mean remanence of the crustal sequence from this and previous studies. While t~~The declination of the reference direction ~~follows~~ is inferred from the geocentric axial dipole (GAD) hypothesis ~~(~~–i.e., the time-averaged declination of the magnetic field points towards the geographic north pole~~)~~–, and is therefore D = 000°. ~~its~~ The inclination of the reference direction has been calculated by combining all the existing (not remagnetized) paleomagnetic data from the layered gabbros and the extrusive sequence (Perrin et al., 2000; Shelton, 1984; Weiler, 2000), including the results ~~obtained from this study~~ from the two pillow basalt sites in this study ~~(Figure S1)~~. The tilt corrected mean inclination calculated from this dataset, representing the inclination of the reference direction, is 21.5° ± 6.6° (Figure S1). ~~Based on these data the reference direction used for the net tectonic rotation analysis in this study has a declination (D) of 000° and inclination (I) of 21.5° ± 6.6°.~~

A set of net tectonic rotation solutions is expressed as (i) azimuth and plunge of the rotation axis, (ii) magnitude and sense of the rotation, and (iii) initial strike of the unit. When applied to vertical units like dykes, two permissible sets of net tectonic rotation solutions are obtained if the dykes can be restored to the vertical. In this case, three selection criteria are used to choose the preferred solution at each site: (1) the calculated rotation has to restore the units to their current position (e.g., a solution yielding overturned beds when units are just gently dipping should be

discarded); (2) both the rotation sense and magnitude have to be consistent with the known regional and/or local deformation pattern; (3) multiple sites within a relatively small area have to show similar net tectonic rotation parameters (assuming local rotations are minor).

One set of solutions is instead obtained when dykes are not restored to vertical (e.g., because they did not intrude vertically). Single solutions are geologically meaningless and should be discarded as both the initial dyke orientation and the rotation parameters will only depend on the orientation of the reference direction (e.g., the initial dyke orientation will always strike perpendicular to the reference direction, hence will always be E-W).

Once a preferred solution has been chosen, an iterative net tectonic rotation analysis (Morris et al., 1998; Koymans et al., 2016) is then used to model the uncertainties on the reference direction (only its inclination), the site mean direction, and the dyke orientation. This routine within the net tectonic rotation analysis package is available at www.paleomagnetism.org and produces at each site 75 permissible solutions per set of solutions (hence 150 when dykes are restored to vertical).

Field Code Changed

Formatted: Hyperlink, Font: +Body, 12 pt, Font color: Auto

4. Results

4.1 Magnetic carrier analysis

Temperature variation of the magnetic susceptibility (Figure 2) is irreversible, with susceptibility values being commonly lower after heating, hence showing mineralogical transformations induced by the experiments. These transformations ~~do not seem to~~did not produce new mineralogical phases, as the Curie temperatures for the heating and cooling curve are the same. On the other hand, in the pillow lavas (site MA01; Figure 2) variable Curie temperatures are inferred from the heating and cooling paths. Curie temperatures of 570-580°C are observed within the dyke samples (Figure 2), indicating nearly pure magnetite as magnetic carrier (Dunlop and Özdemir, 1997). Sites DA and HA show additional Curie temperatures between 300° and 330° (Figure 2), which is consistent with a minor occurrence of iron sulphides, likely pyrrhotite. If present, the break-down of iron sulphides expected during heating at ~500°C (Dunlop and Özdemir, 1997) did not produce any new magnetite as our experiments were conducted in argon atmosphere, hence in reducing conditions. This would explain the lower susceptibility values of the cooling curves in all sites (except site AS where new magnetite might indeed have formed during the experiment; Figure 2). The removal of iron sulphides ~~This~~ during the heating is further ~~suggested~~ supported by the absence of inflections in the cooling paths around 300-330° (Figure 2)~~, as iron sulfides commonly break down to magnetite at about 500°C (Dunlop and Özdemir, 1997)~~. Site AS shows a slightly higher Curie temperature of 595°C, ~~revealing~~ suggesting the occurrence of partly oxidized (maghemitized) magnetite ~~or titanomagnetite~~, common in mafic magmatic rocks (Dunlop and Özdemir, 1997). Pillow lavas from site MA01 show two ~~a primary~~ Curie temperatures of ~~of~~ ~545°C~~,~~ and ~~a possible additional temperature of~~ ~450°C,

compatible with the occurrence of both Ti-poor and Ti-rich titanomagnetite, respectively. , which after heating are converted into titanomaghemite (with Curie temperatures of 520° and 620°C, respectively). Similar blocking temperatures have also been observed at all sites during the thermal demagnetization experiments, confirming the occurrence of magnetite, titanomagnetite, and (titano)maghemite as main carriers of the magnetization in the samples dykes and lavas.

Relatively narrow to more open hysteresis loops characterize all the dyke samples (Figure 3), indicating the predominance of pseudo-single-domain (PSD; 0.05-3 μm) and perhaps minor single-domain (SD; < 0.05 μm) grains (Dunlop and Özdemir, 1997). On the other hand, pillow lava samples show very narrow hysteresis loops (Figure 3), which are typically observed in rocks dominated by multidomain (MD; >3 μm) ferromagnetic grains (Dunlop and Özdemir, 1997).

Ten thin sections from both dykes and pillow lavas were analyzed. The main mineralogical assemblage in dykes is, in order of abundance, plagioclase, clinopyroxene, orthopyroxene, chlorite, and opaque minerals. In some dyke samples (sites AA and HU) opaque minerals are as large as 0.1-0.2 mm. Pillow lavas are much more weathered and altered than the dykes, with most of plagioclase and pyroxene minerals losing their original habit and forming a homogenous, fine grained isotropic matrix. The microscopic fabric of both dykes and pillow lavas is purely magmatic, with frequent euhedral plagioclase and pyroxene minerals (more frequently commonly observed in dykes) forming a matrix with no internal fabric. The opaque minerals are also randomly dispersed within this matrix. Chlorite, which is always present in all the samplesboth dykes and pillow lavas, occurs

randomly dispersed within the isotropic matrix, suggesting a static metamorphism likely associated to seafloor hydrothermal alteration, as frequently observed in other ophiolites (e.g., Maffione et al., 2017). Such metamorphism occurs at very low temperatures and normally does not affect the magnetic remanence ~~recorded~~ of ~~by these~~ rocks emplaced at a mid-ocean ridge~~. Furthermore, seafloor hydrothermal metamorphism only occurs at the spreading ridge during the magmatic phase, hence any potential remagnetization caused by this process would produce a magnetization sub-parallel to the primary remanence.~~

SEM analysis and EDX characterization (Figure 4), revealed the occurrence of angular magnetite and titanomagnetite, sometimes with exolution lamellae, with grain sizes variable between 1 μm (pseudo-single-domain – PSD) and 100 μm (multidomain – MD). At few samples from sites FF and AS, iron~~Fe~~- and titanium~~Ti~~-rich oxides up to 1 mm in size and showing compositional bands have been observed and interpreted as ilmenite. This is supported by the fact that the magnetization of samples carrying such large ilmenite minerals (which is not magnetic) is comparable to that of other samples~~, because these do not seem to contribute to the remanence (which is comparable to that of other samples where these large crystals are not present)~~.

4.2 Paleomagnetic results

Natural remanent magnetization (NRM) intensity from 380 analyzed samples varies between several 10s of mA/m and 4 A/m, suggesting substantial variations in ferromagnetic mineral concentration across the sampled rocks. A total of 340

characteristic remanent magnetizations (ChRMs) were interpreted from the 380 analyzed samples, with the remaining 40 samples showing noisy, uninterpretable demagnetization diagrams, or MAD values above the chosen threshold of 10°.

AF demagnetization diagrams show two components of magnetization: a low-coercivity viscous component usually removed at 10-15 mT, and a stable high-coercivity component isolated within an interval between 20 and 100 mT (Figure 5). At about half of the samples, these high-coercivity components were isolated using great circle fitting (McFadden and McElhinny, 1988), which denoted the occurrence of high-coercivity phases that could not be removed at 100 mT. We suspect this effect might~~to~~ be associated with partial maghemitization of the original magnetite, which causes a slight increase of coercivity. Although this hypothesis remains a valid explanation for the remanence behavior, is not supported by thin section microscope analyses. This might be due to the fact that cracks associated with maghemitization of original (titano)magnetite can sometimes be difficult to identify in thin section.

Overall, AF demagnetization treatment was more effective in isolating the ChRM components (Figure 5), and produced more stable demagnetization components compared to the thermal demagnetization technique (Figure 5E). Nevertheless, the ChRM directions determined from both AF and thermally demagnetized twin specimens are fully consistent (Figure 5C), showing that these are high-stability, likely primary remanence components suitable for tectonic interpretations.

Site mean directions (*in situ* coordinates) at 10 out of 12 sites (Figure 6; Table 1) are significantly different from the present-day GAD field direction at the mean latitude of the Oman ophiolite (D/I = 000°/42°), hence ruling out any recent remagnetization. The remaining two sites (AA and MU) show northerly mean directions that are very close to the expected inclination of the present-day GAD, suggesting possible recent remagnetization (Figure 6; Table 1). For now, this remagnetization cannot be confirmed based on this evidence alone and therefore we use all sites for the net tectonic rotation analysis. ~~These sites were rejected due to possible recent remagnetization.~~ At site HU, several ChRM directions that are close to the present-day GAD direction were discarded due to possible recent remagnetization before computing the site mean direction.

Besides sites AA and MU with northerly directions, the other ten sites show ~~The~~ *in situ* site mean directions ~~from these ten sites are consistent and vary~~varying between southeastward, ~~and~~ northeastward, and northwestward directions~~, with the exception of site BB, which has a northwestward trend~~ (Figure 6; Table 1). The tilt-corrected mean direction from the two combined ~~Because the Oman ophiolite formed during the Cretaceous Normal Superchron (~125-83 Ma) its primary remanences are expected to have a normal polarity (i.e. positive inclinations). While moderate local tilt may account for the reverse polarity of the in situ direction calculated at site DA (Figure 6), the reverse polarity of site BB is more difficult to explain, as it would require a much larger tilt (>150°). Since such extreme deformation has never been documented in the Oman ophiolite, we infer a probable remagnetization at site BB, consistent with a well-documented remagnetization~~

~~event affecting the southeastern massifs of the ophiolite (in which site BB is located) (Feinberg et al., 1999; Morris et al., 2016). Site BB was excluded from further analysis.~~

~~The~~ pillow lava sites (MA01 and MA02) has D = 093.4° and I = 15.9°, and indicates ~~yielded~~ a vertical axis rotation of 93.4° CW ~~in tectonic coordinates~~ (~~MA01 and MA02 combined;~~ Table 1). This is consistent with previous results (Morris et al., 2016; Perrin et al., 2000) indicating large CW rotation of the whole ophiolite, and provides a first-order approximation for ~~of~~ the vertical axis rotation component expected at the other ~~contributing to the net rotation~~dyke sites.

Fold tests to check the primary nature of the interpreted ChRMs cannot be performed in units lacking paleohorizontal control such as dykes. Similarly, fold tests could not be performed ~~for~~on the two pillow lava sites, as rocks there are part of the same outcrop and have the same orientation. In this case VGP distribution may be used to assess the primary nature of the remanence based on the criteria suggested by Deenen et al. (2011).~~However, we observe that the~~ VGP scatters at all the ~~nine~~ sites except HA and is consistent with the expected scatter induced by paleosecular variation (A_{95min}<A_{95}<A_{95max}~~interpreted to carry a primary magnetization (~~; Figure 6 and~~;~~ Table 1).~~ are consistent with the expected scatter induced by paleosecular variation (A_{95min}<A_{95}<A_{95max})~~ The scatter of ChRMs at site HA is smaller than that produced by secular variation (i.e., $A_{95} < A_{95min}$~~;~~ Table 1), yet, this~~-~~ may be explained by the fact that the majority of the remanence directions (i.e., 18 out of 30) at this site have been computed using great circles analysis (McFadden and McElhinny, 1988). Although mathematically and statistically reliable, these

directions do not necessarily replicate the natural scatter of the directions due to secular variation of the geomagnetic field. ~~So~~Therefore, based on the above evidence and in the absence of other constraints to assess the nature of the remanence, we assume for now that the remanence at all sites could be primary.~~Following reliability criteria of Deenen et al. (2011), we conclude that the isolated remanences at these nine sites are primary and use these for the net tectonic rotation analysis.~~

4.3 Net Tectonic Rotation analysis

Net tectonic rotation analysis of the ten ~~of~~ sheeted dyke sites ~~exposed at seven sites~~ succeeded in restoring both the dykes back to their original (vertical) orientation and the computed in situ paleomagnetic directions to the chosen reference direction, generating two sets of permissible solutions at each site (Table 2). Because the Oman ophiolite underwent an overall large (up to 150°) CW vertical axis ~~block~~ rotation (see Morris et al. (2016) for a comprehensive review), preferred solutions were selected among those satisfying all the three criteria listed in the Methods section. Based on these criteria, site BB was discarded as both solutions indicated large CCW rotations, which are at odds with the regional CW rotation of the ophiolite. This might be explained by the fact that the primary remanence at site BB ha~~ves~~ been overprinted, hence giving meaningless net tectonic rotation solutions. This hypothesis is supported by the fact that site BB is within the southern domain of the Oman ophiolite that has been affected by remagnetization during the obduction stage (Morris et al., 2016).

Net tectonic rotation analysis at site MU provided two solutions, one of which is clearly meaningless ~~because giving~~for it gives extremely large CCW rotations. The other set of solutions indicates a CW rotation but the vertical-axis component of ~~such~~this net rotation is quite small and therefore not consistent with the regional large rotation of the ophiolite. Because the in situ remanence of site MU is~~are~~ close to the present-day field (Table 1 and Figure 6), it is indeed likely that this site has been (totally or partially) affected by recent remagnetization. We therefore will not consider the result from this site for further analysis.

Net tectonic rotation analysis at site AA provided two solutions, one producing a CCW rotation (hence discarded) and the other a CW rotation that is potentially consistent with the regional deformation pattern. The rotation pole for this potential preferred solution is between and similar, within error, to both the reference direction and the site mean remanence direction (Table 2). As pointed out by Allerton and Vine (1987), in this circumstance the error associated with the calculation of the net tectonic rotation parameters might be very high. Although all the parameters for this (potentially) preferred solution are consistent with the other sites, we prefer to adopt a conservative approach and discard this site from further analysis.

Preferred solutions could instead be selected at the remaining ~~yielding clockwise rotations along steep axes, and resulting in the largest component of vertical axis rotation (e.g., among solutions providing equal rotation magnitudes those having the steeper axes were chosen as preferred). These criteria allowed us to identify preferred net tectonic rotation solutions at~~ seven sites (Table 2). In

particular, at sites AS, HA, and GD the preferred solutions are those giving CW rotations (while the alternate solutions provided CCW rotastions). The net tectonic rotation analysis for the remaining four sites DA, FF, HD, and HU yielded CW rotations at both sets of solutions. At sites FF, HD, and HU, the preferred solutions have been selected among those giving the largest vertical-axis rotation (the alternative solutions have shallower axes and smaller net rotations that result in minimum vertical axis rotations, which are incompatible with the large rotation observed regionally). Both solutions at the remaining site DA produce an equal amount of vertical axis rotation, yet the alternate (i.e., rejected) solution together with vertical axis rotation produces overturned units, which is not compatible with the overall gentle tilt of the ophiolite (Nicolas et al., 2000).

For these seven preferred solutions~~sites~~ we have then modeled the uncertainties associated with the mean paleomagnetic direction, the dyke orientation, and the reference direction (Figure 7; Table 2). The rotation axes at these seven sites are moderately to steeply plunging approximately to the west (sites AS, FF, and GD), to the north-northeast (sites HA, HU, and HD), and to the southeast (site DA). The rotation magnitude is variable between ~80° and ~160°, consistent with the large regional rotation of the ophiolite (Morris et al., 2016). There seems to be no correlation between the orientation of the rotation axes or the magnitude of the net rotations and the location of these seven sites.

The calculated initial dyke strike is consistently NNE to ENE (Table 2 and Figure 7). When the modeled initial dyke orientations from all seven sites are plotted together (525 directions), the ~~main (~~most frequent~~ solution)~~ initial

strike~~trend~~ of the sheeted dykes at the scale of the whole ophiolite is NNE-SSW, ~~striking~~ between 020° and 030° (Figure 7). A bimodal distribution seems to appear in this diagram, with primary NNE-SSW and secondary ENE-WSW directions. We consider the predominant (more frequent) NNE-SSW trend as representative of the direction of the spreading ridge at which these dykes were emplaced in the Cretaceous. The ENE-WSW directions, if meaningful, may be related to dykes locally intruded at an angle to the NNE-SSW trending spreading ridge, or to an artifact of the modeling.

5. Discussion

Our results indicate that the oceanic crust of the Oman ophiolite accreted at a NNE-SSW trending spreading center, which, given the geochemical and geochronological evidence was located in the upper plate above an infant subduction zone (Guilmette et al., 2018; MacLeod et al., 2013; Rioux et al., 2016). Interestingly, regardless of the geochemical signature of the ophiolitic crust, the orientation of this spreading center already makes it quite unlikely that the crust of the Oman ophiolite formed at the Neotethyan mid-oceanic ridge as suggested before (e.g., Nicolas et al., 2000): the overall strike of the Gondwana passive margins, and hence of the Neotethys ridge, was NW-SE rather then ~NNE-SSW (in Cretaceous paleomagnetic coordinates) (Figure 8b).

The location, in present-day coordinates, of the subduction zone above which the Oman ophiolite was formed is best estimated from the modern obduction front

in the western and southern edge of the ophiolite, although post-obduction erosion may have removed some of the most trench-proximal parts of the ophiolite. The sheeted dyke sections strike approximately sub-parallel to this obduction front, suggesting that the spreading occurred orthogonal to the trench. This is further suggested by the narrow, 96-95 Ma age range of the ophiolitic crust along the ophiolite's strike (Rioux et al., 2016). Such a narrow age range is expected when a fast-spreading ridge is located parallel to the subduction front. Upon spreading, this supra-subduction zone ridge migrates away from the trench at half-spreading rate. With spreading rates of 5-10 cm/yr estimated for the Semail ophiolite (Rioux et al., 2016), and an exposed width orthogonal to the obduction front of <100 km, only 1-2 Myr worth of ophiolite spreading history can be preserved in the modern ophiolite, whereas all crust that accreted due to younger spreading must be located offshore northern Oman (Figure 8d). Had spreading occurred parallel to the trench, the 500 km long ophiolite should have had crustal ages spanning 5-10 Myr from north to south (Maffione et al., 2017). We therefore conclude that the subduction zone above which the Oman ophiolite accreted was also striking NNE-SSW, parallel to the restored dyke orientation.

A NNE-SSW original orientation of the ophiolite is fully consistent with the vertical axis rotations estimated from paleomagnetic data (Morris et al., 2016) suggesting that the ophiolite underwent up to ~150° clockwise rotation between the formation of its crust at ~96-95 Ma, and the end of obduction around 70 Ma (Morris et al., 2016). Back-rotating the ophiolite around its modern northwestern tip to its original NNE-SSW strike provides the minimum horizontal displacement

between subduction initiation and obduction. Such a rotation, along a small circle at the ophiolite's southeastern tip, involves a total horizontal motion relative to Arabia of ~1000 km. This gives an average long-term drift rate of ~4 cm/yr, which is well within the ranges of similar strongly rotating trenches that roll back along and obduct passive margins (e.g., Chertova et al., 2014). This restoration places the ophiolite's northern (i.e. modern eastern) tip at a paleolatitude of ~5°N. Paleolatitudes calculated from the ophiolite's crust allow for a somewhat more northerly paleolatitude for ophiolite spreading, and the plate motion rates during ophiolite-Arabia convergence may thus have been somewhat higher. Nevertheless, this analysis shows that the ultra-high spreading rates inferred based on U/Pb crustal ages (Rioux et al., 2016) must have been short-lived, focused in the period of inception of upper plate spreading.

Perrin et al. (2000) showed rapid clockwise rotations during ophiolite formation, from major declination differences within the effusive sequence. Whilst the rotation sense and magnitude of these rotations are consistent with the total rotation of the whole ophiolite, the short time span during which the effusive rocks accumulated of only a few million years makes it unlikely that these rotations represent the rotation of the entire ophiolite: if they were representative, these would require plate motion and subduction rates of up to meters per year, which is geodynamically unrealistic. We therefore infer that the results reported in Perrin et al. (2000) reflect tectonic deformation within the ophiolite, e.g. along transform faults, which may cause local rotation, as observed in the Troodos ophiolite of Cyprus (Morris and Maffione, 2016).

Our reconstructed initial trench orientation associated with the Semail ophiolite now allows assessing the nature of the weakness zone at which subduction initiated – the main aim of our study. A NNE-SSW original strike of the subduction zone is approximately orthogonal to the Arabian passive continental margin at ~95 Ma, when corrected for plate motions in a paleomagnetic reference frame (Torsvik et al., 2012). Weakness zones expected in such an orientation are likely to be fracture zones. This conclusion for the Semail ophiolite does not come in isolation: coeval ophiolites from Cyprus, Syria, and Turkey all share a similar ridge and inferred trench orientation, and also in those settings, trenches and supra-subduction zone ridges were striking N-S to NE-SW, orthogonally to restored passive margins (Maffione et al., 2017) (Figure 8b). Moreover, such a former fracture zone orientation is preserved in the Arabian margin today along the N-S striking coast of northern Oman and the UAE, connecting passive margins of northeast Oman, and the restored margin of the Zagros mountains in Iran (Figure 8b). It thus appears that Cretaceous subduction initiation in the Neotethys Ocean was driven by (ES)E-(WN)W contraction, rather than the widely inferred ~N-S convergence. This may help in our search for the potential drivers of subduction initiation.

When the underthrusting of the Arabian passive margin at the Zagros collision zone of Iran is restored (McQuarrie and van Hinsbergen, 2013), the original Oman-UAE fracture zone margin, of Permian age (Béchennec et al., 1990; Stampfli and Borel, 2002), extended several hundreds of kilometers farther to the north than today (Figure 8b). We restore the original orientation of the ophiolite, and of the

newly formed subduction zone at which the ophiolite's sole started forming just before 104 Ma, adjacent to this ancient Arabian continent-parallel fracture zone. The initiation probably occurred sufficiently far east of the margin to be in an intra-oceanic setting, since no continental crust relics are found in the ophiolite, but nevertheless close to that continental margin.

Near-continental margin intra-oceanic subduction initiation and formation of supra-subduction zone ophiolites was restored for the Indus-Yarlung ophiolites of southern Tibet (Maffione et al., 2015b). There, it was thus already inferred that supra-subduction zone ophiolites are not necessarily associated with subduction initiation in the vicinity of a mid-ocean ridge. In this study, we propose a similar scenario for the Semail ophiolite, where mid-ocean ridge inversion has long been the preferred model (Boudier et al., 1988; Duretz et al., 2016). Our reconstruction places Arabian lithosphere in the upper plate, but even if subduction initiated farther to the northeast such that oceanic crust adjacent to the Zagros margin was located in the upper plate, it is quite unlikely that an active ridge was present there at that time. Active mid-ocean ridges are commonly not observed in the vicinity of a 170 Myr old passive margin, and as pointed out by Maffione et al. (2017), it is unlikely that the Cretaceous Neotethys ocean between Arabia and Eurasia still contained an active mid-ocean ridge: the ridge at which the Neotethys opened would have long subducted below the Iranian active margin by that time (such as inferred by Stampfli and Borel (2002)). We may thus infer that, in absence of an active mid-ocean ridge in an ocean, passive margins, or fracture zone margins, may be the preferred locus of subduction initiation.

Such settings of continental margin-parallel fracture zones are today abundant along the west and east coast of Africa (Figure 8a). Recent studies have shown through seismic interpretation that the fracture zone margin of west Africa was associated with hyperextension and exhumation of serpentinized mantle during continental breakup (Gillard et al., 2017). Serpentine-rich faults along hyperextended margins are weak and may localize subduction initiation upon forced convergence (Maffione et al., 2015a). We envisage that such a setting may have facilitated subduction initiation in the Oman case, although we note that the old age of this setting at the time of subduction initiation (~170 Myr) renders it likely that a thick, unbroken lithospheric mantle was present, whose strength must be overcome to initiate subduction.

Our results, and those of Maffione et al. (2017) for the Mediterranean region, raise several first-order new questions for understanding subduction initiation dynamics. Our results show that Cretaceous subduction initiation within the Neotethys ocean formed a new plate (the Anadolu plate of Gürer et al. (2016) separated from Eurasia and Africa-Arabia by trenches (Figure 8). This plate must have moved westward relative to Africa/Arabia (and Eurasia, given overall N-S Africa-Eurasia convergence) to drive subduction initiation along N-S striking trenches. Gaina et al. (2015) showed based on Indian Ocean reconstructions that prior to the end of the Cretaceous superchron, India rotated counterclockwise relative to Arabia that requires such convergence. Did the driver of this rotation also spark subduction initiation farther westwards? And what processes cause the hot conditions recorded in the Oman metamorphic sole 8 Myr of upper plate spreading

(Guilmette et al., 2018) with subduction initiating in old, cold lithosphere? We refrain from speculating on these questions, but leave these for future study and debate.

6. Conclusions

The subduction zone above which the crust of the Semail ophiolite of Oman formed is widely thought to have initiated along, or in the vicinity of a Neotethyan mid-oceanic ridge. In this paper, we restored the paleo-orientation of the supra-subduction zone ridge at which the Semail ophiolitic crust accreted around ~96-95 Ma, through paleomagnetic analysis of its sheeted dyke sections. Our results from seven localities covering the entire width of the ophiolite consistently show that this ridge was orientated NNE-SSW. We infer that the trench orientation, marked by the modern obduction front, was oriented sub-parallel to this trench. Our results thus indicate that the trench orientation was approximately orthogonal to the Arabian passive margin. We infer that subduction initiated along a fracture zone that was located parallel to, and likely in the vicinity of, the fracture zone that connected the Permian Arabian passive margin of northern Oman with the margin underthrust below Iran at the Zagros collision zone. This places Arabian continental crust in the upper plate during subduction initiation. Subduction hence did not initiate in the vicinity of the Neotethyan ridge, which according to plate reconstructions had long been subducted during Cretaceous subduction initiation. We conclude that subduction was induced by (ES)E-(WN)W contraction, as previously also inferred

for ophiolite belts of the eastern Mediterranean and NW Arabian margins. This may help the future identification of the dynamic trigger of subduction initiation in the Neotethys Ocean.

Acknowledgements

DJJvH acknowledges a Netherlands Organization for Scientific Research (NWO) VIDI grant 864.11.004. CG acknowledges a NSERC-DG grant #RGPIN-2014-05681. We thank Benoit Charette for field assistance.

Figure Captions

Figure 1. Geological map of the Oman ophiolite.

Figure 2. High-temperature variations of low-field magnetic susceptibility (k) for six representative samples (five from dykes and one from pillow lavas). Diagrams are mainly irreversible, showing mineralogical transformation during heating. Curie temperatures have been inferred from the heating paths.

Figure 3: Hysteresis loops for six representative samples (the same as in Figure 2), showing predominantly narrow to slightly open loops typical of multidomain (MD) magnetic grains.

Figure 4: Back-scattered electron (BSE) images of representative thin sections from sheeted dykes showing the presence of iron oxides (magnetite, titanomagnetite, and possibly ilmenite) with variable size from ~1 μm to ~1 mm.

Figure 5: A-F - Representative orthogonal vector plots (Zijderveld diagrams) of both alternating field and thermal demagnetization for various sites (in situ coordinates). C – An example of consistent ChRM directions acquired in AF and TH demagnetized sister samples. NRM = natural remanent magnetization. Steps are shown in °C or mT.

Figure 6. Stereographic projections of the interpreted characteristic remanent magnetization directions (ChRMs) and virtual geomagnetic poles (VGPs) from all sites. The great circles used in the principal component analysis are shown in the left diagrams (dotted curve), together with the direction isolated from these~~using best-fit lines~~ (small black dots). The middle ChRM plots show all the ChRM directions calculated from best-fit lines and great circle analysis (blue dots = normal polarity; open dots = reverse polarity; gray dots = discarded direction after 45° cut-off). The red ellipse is the cone of confidence around the computed mean direction, while the light blue shaded area is the error on the mean declination (ΔD in Table1). The VGP plots o~~i~~n the right of each site show the accepted VGPs (blue dots) and the discarded VGPs (gray dots), which in fact fall outside the solid inner circle that represents the 45° cut-off. The Grea~~a~~y star in the left plots is the present-day GAD field direction.~~The poles calculated from the great circles are then shown in the diagrams in the middle.~~

Figure 7. (Left) Stereographic projections of the permissible initial dyke orientations (rose diagram) and rotation poles calculated after modeling of the uncertainties associated to the input vectors of the net tectonic rotation analysis, following methods of Morris et al. (1998) and Koymans et al. (2016). (Right) Frequency distribution of the permissible rotation magnitude obtained from the same analysis. Summary plots showing the mean initial dyke orientation and rotation magnitude are shown in the bottom right corner, and have been obtained by combining all the permissible results from the seven sites.

Figure 8. Tectonic model of subduction initiation along the Arabian margin of Oman. Reconstruction of continents in paleomagnetic reference frame of Torsvik et al. (2012). Reconstruction of the Zagros margin following McQuarrie and van Hinsbergen (2013), and of eastern Mediterranean subduction initiation and obduction following Maffione et al. (2017). A) Fracture zone and passive margins of the modern African continent, providing a modern example of the restored Arabian-Greater Adria continental margin, where the fracture zone margins were the locus of Cretaceous subduction initiation. Basic plate kinematics requires that the N-S subduction segments were connected with a transform fault parallel to (and here dotted along) the Arabian passive margin. B-D) Subduction initiation parallel and close to the Oman-UAE fracture zone margin around 105 Ma is followed by forearc extension around 96-95 Ma, and subsequent rotation of the forearc Oman ophiolite, followed by ~70 Ma obduction. Bey = Bey Dağları Platform; Kir = Kırşehir Massif, Tav = Tavşanlı Zone; for the tectonic history of the eastern Mediterranean region, see Gürer et al. (2016) and Maffione et al. (2017).

Table 1: *Remagnetized sites. [A] In situ directions. [B] Tilt corrected directions. Lithologies are sheeted dykes (SD) and pillow lavas (PL). δDipDir is the 95% confidence around the mean pole to dyke measured in the field. (N meas.) is the number of dykes measured in the field to calculate the mean direction. ChRM interpretation has used best-fit lines (L) and great circles (GC) fitting. n/N is the number of specimens used in the statistics over the total number of analysed

samples. D, dDx, I, dIx are declination and associated error, and inclination and associated error. α_{95} = semiangle of the 95% cone of confidence around the site-mean ChRM direction (Fisher, 1953). K is Fisher's precision parameter relative to the ChRMs (Fisher, 1953). A_{95} is the semiangle of the 95% cone of confidence around the mean virtual geomagnetic pole (VGP). K is Fisher's precision parameter relative to the VGPs. A_{95min} and A_{95max} are the minimum and maximum semiangle of the 95% cone of confidence expected for the given dataset by paleosecular variation.

Table 2: Results of the net tectonic rotation analysis (Allerton and Vine, 1987) showing the calculated values for the azimuth and plunge of the rotation axis, rotation magnitude and sense, and restored dyke strike and plunge. Reference direction used: D = 000°, I = 21.5° ± 6.6°. In situ dyke orientations and associated uncertainties used for the analysis are in Table 1. Two sets of solutions have been obtained at each site and identified as "preferred" (the one used for the tectonic interpretation) and "alternate" (the one discarded).

Supplementary files: Data (.dir) and statistical interpretation (.pmag) files of the paleomagnetic data that lie at the basis of this paper. Data can be viewed and analyzed at www.paleomagnetism.org (Koymans et al., 2016).

7. References

Agard, P., Jolivet, L., Vrielynck, B., Burov, E., Monié, P., 2007. Plate acceleration: The obduction trigger? Earth and Planetary Science Letters 258, 428-441.

Agard, P., Yamato, P., Soret, M., Prigent, C., Guillot, S., Plunder, A., Dubacq, B., Chauvet, A., Monié, P., 2016. Plate interface rheological switches during subduction infancy: Control on slab penetration and metamorphic sole formation. Earth and Planetary Science Letters 451, 208-220.

Allerton, S., Vine, F., 1987. Spreading structure of the Troodos ophiolite, Cyprus: Some paleomagnetic constraints. Geology 15, 593-597.

Béchennec, F., Le Métour, J., Rabu, D., Bourdillon-de-Grissac, C., De Wever, P., Beurrier, M.t., Villey, M., 1990. The Hawasina Nappes: stratigraphy, palaeogeography and structural evolution of a fragment of the south-Tethyan passive continental margin. Geological Society, London, Special Publications 49, 213-223.

Boudier, F., Ceuleneer, G., Nicolas, A., 1988. Shear zones, thrusts and related magmatism in the Oman ophiolite: initiation of thrusting on an oceanic ridge. Tectonophysics 151, 275-296.

Chertova, M.V., Spakman, W., Geenen, T., van den Berg, A.P., and van Hinsbergen, D.J.J., 2014. Underpinning tectonic reconstructions of the western Mediterranean region with dynamic slab evolution from 3-D numerical modeling. Journal of Geophysical Research 119, 5876-5902.

Formatted: Font: 12 pt

Formatted: Font: 12 pt

Formatted: Font: 12 pt

Formatted: Font: 12 pt

Formatted: Font: 12 pt

Formatted: Font: 12 pt, Not Italic

Formatted: Font: 12 pt

Formatted: Font: 12 pt

Cowan, R.J., Searle, M.P., Waters, D.J., 2014. Structure of the metamorphic sole to the Oman Ophiolite, Sumeini Window and Wadi Tayyin: implications for ophiolite obduction processes. Geological Society, London, Special Publications 392, 155-175.

Deenen, M.H.L., Langereis, C.G., van Hinsbergen, D.J.J., Biggin, A.J., 2011. Geomagnetic secular variation and the statistics of palaeomagnetic directions. Geophysical Journal International 186, 509-520.

Dunlop, D.J., Özdemir, Ö., 1997. Rock magnetism: fundamentals and frontiers. Cambridge university press.

Duretz, T., Agard, P., Yamato, P., Ducassou, C., Burov, E.B., Gerya, T.V., 2016. Thermo-mechanical modeling of the obduction process based on the Oman Ophiolite case. Gondwana Research 32, 1-10.

Ernewein, M., Pflumio, C., Whitechurch, H., 1988. The death of an accretion zone as evidenced by the magmatic history of the Sumail ophiolite (Oman). Tectonophysics 151, 247-274.

Feinberg, H., Horen, H., Michard, A., Saddiqi, O., 1999. Obduction-related remagnetization at the base of an ophiolite: Paleomagnetism of the Samail nappe lower sequence and of its continental substratum, southeast Oman Mountains. Journal of Geophysical Research: Solid Earth 104, 17703-17714.

Fisher, R., 1953. Dispersion on a sphere. Proceedings of the Royal Society of London. Series A. Mathematical and Physical Sciences 217, 295-305.

Gaina, C., van Hinsbergen, D.J.J., Spakman, W., 2015. Tectonic interactions between India and Arabia since the Jurassic reconstructed from marine geophysics, ophiolite geology, and seismic tomography. Tectonics 34, 875-906.

Gillard, M., Sauter, D., Tugend, J., Tomasi, S., Epin, M.E., Manatschal, G., 2017. Birth of an oceanic spreading center at a magma-poor rift system. Sci Rep 7, 15072.

Godard, M., Bosch, D., Einaudi, F., 2006. A MORB source for low-Ti magmatism in the Semail ophiolite. Chemical Geology 234, 58-78.

Guilmette, C., Smit, M.A., van Hinsbergen, D.J.J., Gürer, D., Corfu, F., Charette, B., Maffione, M., Rabeau, O., Savard, D., 2018. Forced subduction initiation recorded in the sole and crust of the Semail ophiolite, Oman. Nature Geoscience 11, ~~in press~~688-695.

Gürer, D., van Hinsbergen, D.J.J., Matenco, L., Corfu, F., Cascella, A., 2016. Kinematics of a former oceanic plate of the Neotethys revealed by deformation in the Ulukışla basin (Turkey). Tectonics 35, 2385-2416.

Hacker, B., Mosenfelder, J., Gnos, E., 1996. Rapid emplacement of the Oman ophiolite: Thermal and geochronologic constraints. Tectonics 15, 1230-1247.

Hacker, B.R., 1991. The role of deformation in the formation of metamorphic gradients: ridge subduction beneath the Oman ophiolite. Tectonics 10, 455-473.

Hacker, B.R., Gnos, E., 1997. The conundrum of Samail: explaining the metamorphic history. Tectonophysics 279, 215-226.

Hall, C.E., Gurnis, M., Sdrolias, M., Lavier, L.L., Müller, R.D., 2003. Catastrophic initiation of subduction following forced convergence across fracture zones. Earth and Planetary Science Letters 212, 15-30.

Formatted: Font: 12 pt
Formatted: Font: 12 pt
Formatted: Font: 12 pt
Formatted: Font: 12 pt
Formatted: Font: 12 pt, Not Italic
Formatted: Font: 12 pt
Formatted: Font: 12 pt
Formatted: Font: 12 pt
Formatted: Font: 12 pt
Formatted: Font: 12 pt
Formatted: Font: 12 pt
Formatted: Font: 12 pt, Not Italic
Formatted: Font: 12 pt
Formatted: Font: 12 pt

Kirschvink, J., 1980. The least-squares line and plane and the analysis of palaeomagnetic data. Geophysical Journal International 62, 699-718.

Koymans, M.R., Langereis, C.G., Pastor-Galán, D., van Hinsbergen, D.J.J., 2016. Paleomagnetism.org: An online multi-platform open source environment for paleomagnetic data analysis. Computers & Geosciences 93, 127-137.

MacLeod, C.J., Johan Lissenberg, C., Bibby, L.E., 2013. "Moist MORB" axial magmatism in the Oman ophiolite: The evidence against a mid-ocean ridge origin. Geology 41, 459-462.

Maffione, M., Thieulot, C., van Hinsbergen, D.J.J., Morris, A., Plümper, O., Spakman, W., 2015a. Dynamics of intraoceanic subduction initiation: 1. Oceanic detachment fault inversion and the formation of supra-subduction zone ophiolites. Geochemistry, Geophysics, Geosystems 16, 1753-1770.

Maffione, M., van Hinsbergen, D.J.J., de Gelder, G.I.N.O., van der Goes, F.C., Morris, A., 2017. Kinematics of Late Cretaceous subduction initiation in the Neo-Tethys Ocean reconstructed from ophiolites of Turkey, Cyprus, and Syria. Journal of Geophysical Research: Solid Earth 122, 3953-3976.

Maffione, M., van Hinsbergen, D.J.J., Koornneef, L.M.T., Guilmette, C., Hodges, K., Borneman, N., Huang, W., Ding, L., Kapp, P., 2015b. Forearc hyperextension dismembered the south Tibetan ophiolites. Geology 43, 475-478.

McFadden, P., McElhinny, M., 1988. The combined analysis of remagnetization circles and direct observations in palaeomagnetism. Earth and Planetary Science Letters 87, 161-172.

McQuarrie, N., van Hinsbergen, D.J.J., 2013. Retrodeforming the Arabia-Eurasia collision zone: Age of collision versus magnitude of continental subduction. Geology 41, 315-318.

Morris, A., Anderson, M.W., Robertson, A.H., 1998. Multiple tectonic rotations and transform tectonism in an intraoceanic suture zone, SW Cyprus. Tectonophysics 299, 229-253.

Morris, A., Maffione, M., 2016. Is the Troodos ophiolite (Cyprus) a complete, transform fault–bounded Neotethyan ridge segment? Geology 44, 199-202.

Morris, A., Meyer, M., Anderson, M.W., MacLeod, C.J., 2016. Clockwise rotation of the entire Oman ophiolite occurred in a suprasubduction zone setting. Geology 44, 1055-1058.

Mullender, T.A.T., Frederichs, T., Hilgenfeldt, C., de Groot, L.V., Fabian, K., Dekkers, M.J., 2016. Automated paleomagnetic and rock magnetic data acquisition with an in-line horizontal "2G" system. Geochemistry, Geophysics, Geosystems 17, 3546-3559.

Nicolas, A., 1989. Structures of ophiolites and dynamics of oceanic lithosphere. Springer Science & Business Media.

Nicolas, A., Boudier, F., Ildefonse, B., Ball, E., 2000. Accretion of Oman and United Arab Emirates ophiolite–discussion of a new structural map. Marine Geophysical Researches 21, 147-180.

Pearce, J.A., Lippard, S.J., Roberts, S., 1984. Characteristics and tectonic significance of supra-subduction zone ophiolites. Geological Society, London, Special Publications 16, 77-94.

Perrin, M., Plenier, G., Dautria, J.-M., Cocuaud, E., Prévot, M., 2000. Rotation of the Semail ophiolite (Oman): additional paleomagnetic data from the volcanic sequence. Marine Geophysical Researches 21, 181-194.

Pourteau, A., Scherer, E.E., Schorn, S., Bast, R., Schmidt, A., Ebert, L., 2018. Thermal evolution of an ancient subduction interface revealed by Lu–Hf garnet geochronology, Halilbağı Complex (Anatolia). Geoscience Frontiers.

Rioux, M., Garber, J., Bauer, A., Bowring, S., Searle, M., Kelemen, P., Hacker, B., 2016. Synchronous formation of the metamorphic sole and igneous crust of the Semail ophiolite: New constraints on the tectonic evolution during ophiolite formation from high-precision U–Pb zircon geochronology. Earth and Planetary Science Letters 451, 185-195.

Searle, M., Cox, J., 1999. Tectonic setting, origin, and obduction of the Oman ophiolite. Geological Society of America Bulletin 111.

Searle, M., Warren, C., Waters, D., Parrish, R., 2004. Structural evolution, metamorphism and restoration of the Arabian continental margin, Saih Hatat region, Oman Mountains. Journal of Structural Geology 26, 451-473.

Shelton, A.W., 1984. Geophysical studies on the northern Oman ophiolite. Open University.

Soret, M., Agard, P., Dubacq, B., Plunder, A., Yamato, P., 2017. Petrological evidence for stepwise accretion of metamorphic soles during subduction infancy (Semail ophiolite, Oman and UAE). Journal of Metamorphic Geology 35, 1051-1080.

Stampfli, G.M., Borel, G., 2002. A plate tectonic model for the Paleozoic and Mesozoic constrained by dynamic plate boundaries and restored synthetic oceanic isochrons. Earth and Planetary Science Letters 196, 17-33.

Stern, R.J., Gerya, T., 2017. Subduction initiation in nature and models: A review. Tectonophysics.

Stern, R.J., Reagan, M., Ishizuka, O., Ohara, Y., Whattam, S., 2012. To understand subduction initiation, study forearc crust: To understand forearc crust, study ophiolites. Lithosphere 4, 469-483.

Torsvik, T.H., Van der Voo, R., Preeden, U., Mac Niocaill, C., Steinberger, B., Doubrovine, P.V., van Hinsbergen, D.J.J., Domeier, M., Gaina, C., Tohver, E., Meert, J.G., McCausland, P.J.A., Cocks, L.R.M., 2012. Phanerozoic polar wander, palaeogeography and dynamics. Earth-Science Reviews 114, 325-368.

van Hinsbergen, D.J.J., Peters, K., Maffione, M., Spakman, W., Guilmette, C., Thieulot, C., Plümper, O., Gürer, D., Brouwer, F.M., Aldanmaz, E., Kaymakcı, N., 2015. Dynamics of intraoceanic subduction initiation: 2. Suprasubduction zone ophiolite formation and metamorphic sole exhumation in context of absolute plate motions. Geochemistry, Geophysics, Geosystems 16, 1771-1785.

Wakabayashi, J., Dilek, Y., 2003. What constitutes 'emplacement' of an ophiolite?: Mechanisms and relationship to subduction initiation and formation of metamorphic soles. Geological Society, London, Special Publications 218, 427-447.

Warren, C.J., Parrish, R.R., Waters, D.J., Searle, M.P., 2005. Dating the geologic history of Oman's Semail ophiolite: insights from U-Pb geochronology. Contributions to Mineralogy and Petrology 150, 403-422.

Weiler, P., 2000. Differential rotations in the Oman ophiolite: paleomagnetic evidence from the southern massifs. Marine Geophysical Researches 21, 195-210.

Zijderveld, J., 1967. AC demagnetization of rocks: analysis of results, Developments in solid earth geophysics. Elsevier, pp. 254-286.

***Highlights (for review)**

- The Semail ophiolite formed along a NNE-SSW striking ridge above a parallel, incipient subduction zone.
- The nascent Semail subduction zone formed orthogonal and close to the Arabian passive margin
- Subduction initiation likely occurred along an ancient, Permian Neotethyan fracture zone.

Kinematic and paleomagnetic restoration of the Semail Ophiolite (Oman) reveals subduction initiation along an ancient Neotethyan fracture zone

Douwe J.J. van Hinsbergen[1], Marco Maffione[1,2], Louise M.T. Koornneef[1,3], Carl Guilmette[4]

1. Department of Earth Sciences, Utrecht University, Heidelberglaan 2, 3584 CS Utrecht, Netherlands
2. School of Geography, Earth and Environmental Sciences, University of Birmingham, B15 2TT, UK
3. School of Geography, Earth and Environmental Sciences, Plymouth University, Drake Circus, PL4 8AA Plymouth, UK
4. Département de Géologie et de Génie Géologique, Université Laval, Québec, QC G1K 7P4, Canada

For: EPSL

Abstract

The archetypal Semail ophiolite of Oman has inspired much thought on the dynamics of initiation of intra-oceanic subduction zones. Current models invoke subduction initiation at a mid-oceanic ridge located sufficiently close to the Arabian passive margin to allow initiation of continental subduction below the ophiolite within ~10-15 Myr after the 96-95 Ma age of formation of supra-subduction zone crust. Here, we perform an extensive paleomagnetic analysis of sheeted dyke sections across the Semail ophiolite to restore the orientation of the supra-subduction zone ridge during spreading. Our results consistently indicate that the ridge was oriented NNE-SSW, and we infer that the associated trench, close to the modern obduction front, had the same orientation. Our data are consistent with a previously documented ~150° clockwise rotation of the ophiolite, and we reconstruct that the original subduction zone was WNW-ward dipping and NNE-SSW striking. Initial subduction likely occurred in the ocean adjacent and parallel to the Arabian transform margin that formed the original underpinnings of rocks in the Zagros fold-thrust belt, now underthrust below Iran. Subduction thus likely initiated along an ancient, continental margin-parallel fracture zone, as also recently inferred from near-coeval ophiolites from the eastern Mediterranean and NW Arabian regions. Subduction initiation was therefore likely induced by (WN)W-(ES)E contraction, and this constraint may help the future identification of the dynamic triggers of Neotethyan subduction initiation in the Late Cretaceous.

1. Introduction

Subduction initiation is a critical step in the plate tectonic cycle, and how and where subduction zones form has therefore been at the forefront of geodynamic research for decades (e.g., Guilmette et al., 2018; Hall et al., 2003; Stern and Gerya, 2017). Ophiolites, i.e. exposed fragments of oceanic lithosphere that are often found thrust upon continental margins, have played a central role in the development of concepts of subduction initiation (Pearce et al., 1984; Stern et al., 2012). First, Pearce et al. (1984), among others, recognized that most ophiolites contain geochemical evidence that indicate formation at a spreading center located above a subduction zone (for this reason called supra-subduction zone (SSZ) ophiolites). Second, many SSZ ophiolites are associated with metamorphic soles - typically high-temperature, low to high-pressure metabasalts and metasediments that are found below the ophiolite's mantle section, thought to have been derived from the top of now-subducted oceanic lithosphere. Their high metamorphic temperatures are atypical for mature, cool subduction zones and metamorphic soles are therefore thought to form at the plate contact during subduction zone infancy (e.g., Agard et al., 2016; Boudier et al., 1988; Guilmette et al., 2018; Hacker and Gnos, 1997; Pourteau et al., 2018; Soret et al., 2017; van Hinsbergen et al., 2015; Wakabayashi and Dilek, 2003). Because both the upper plate - the ophiolite - as well as the down-going plate in these systems are oceanic, as deduced from oceanic lithologies in the metamorphic soles and underlying subduction mélanges, SSZ ophiolites are thought to result from intra-oceanic subduction initiation (Agard et al., 2007; Stern et al., 2012; van Hinsbergen et al., 2015; Wakabayashi and Dilek, 2003).

Models of intra-oceanic subduction initiation logically point at pre-existing weakness zones within oceanic lithosphere as locations where subduction zones may form, either spontaneously or induced (e.g., Agard et al., 2007 ; Guilmette et al., 2018; Stern et al., 2012), at or near active intra-oceanic plate boundaries: transform faults or young fracture zones, ridges, or ridge-parallel detachment faults (Agard et al., 2007; Boudier et al., 1988; Duretz et al., 2016; Hall et al., 2003; Maffione et al., 2015a; Stern et al., 2012; van Hinsbergen et al., 2015).

Along the northern margin of Arabia, and as the highest structural unit in a microcontinent-derived fold-thrust belt in the eastern Mediterranean region, a discontinuous, ~4000 km-long belt of SSZ ophiolites is found with well-constrained crustal ages of ~96-90 Ma (Maffione et al., 2017; Rioux et al., 2016). The best-exposed and most complete of these is the Semail ophiolite of Oman, and has allowed mapping out 100's of km long, coherent fossil ocean floor (e.g., Nicolas et al., 2000). This ophiolite has inspired much thought on the process of subduction initiation and is widely considered to have formed in the incipient stages of an intra-oceanic subduction zone.

Given the overall N-S long-term Arabia-Eurasia plate convergence, subduction is widely considered to have formed along an ~(WN)W-(ES)E striking mid-ocean ridge within the Neotethys (e.g., Duretz et al., 2016). As drivers for subduction initiation, for instance a far-field driven Arabia-Eurasia convergence rate increase of 2-3 cm/yr (Agard et al., 2007) was proposed. However, paleomagnetic constraints from sediments and igneous rocks of the ophiolite indicate that the Oman ophiolite underwent a major, clockwise vertical axis rotation of as much as

150° (e.g., Perrin et al., 2000; Morris et al., 2016). Back-rotating the present-day obduction front (as a proxy for the intra-oceanic trench location) according to these data suggests that the spreading center at which the Oman crust was formed had a NE-SW orientation, hence almost orthogonal to the Arabian passive-margin, not parallel to it. Second, the earliest metamorphism of Arabian passive continental margin rocks found below the Oman ophiolite is dated at ~80-85 Ma old (Warren et al., 2005), i.e. the Arabian passive margin was already buried at the trench only ~10 Myr after supra-subduction zone ophiolite formation. This suggests that subduction initiated close to the Arabian passive margin, as also indicated by paleomagnetic paleolatitudes (Perrin et al., 2000) and incorporated in various numerical and analogue models (Duretz et al., 2016). Opening of the Neotethys ocean and formation of the Arabian passive margin, however, was Permian in age, and thus occurred as much as ~170 Myr prior to Cretaceous subduction initiation (e.g., Béchennec et al., 1990; Stampfli and Borel, 2002). The presence of a Cretaceous mid-ocean ridge close to a Permian passive margin is unlikely, particularly since the original Neotethyan mid-oceanic ridge must have already subducted below the Eurasian margin in Jurassic time (Maffione et al., 2017; Stampfli and Borel, 2002).

In this paper, we provide the first paleomagnetic dataset from the sheeted dyke sections of the Oman ophiolite to kinematically restore the orientation of its SSZ spreading ridge during subduction zone infancy. To this end, we collected a large paleomagnetic data set from ten localities in sheeted dyke sections along the strike of the Oman ophiolite to determine the net rotation history of the ophiolite and restore the dykes to their original orientation. We then place the Oman ophiolite

in plate kinematic context using the configuration of the Arabian passive margin restored for continental subduction in the Zagros mountains (McQuarrie and van Hinsbergen, 2013), cast in a paleomagnetic frame of reference (Torsvik et al., 2012). Finally, we discuss the implications for the tectonic setting and nature of the weakness zone that facilitated Oman's subduction initiation, and search for settings in today's snapshot of plate tectonic history that may provide an analogue.

2. Geological setting

The Semail ophiolite in Oman consists of a large, well-preserved oceanic lithosphere thrust slice containing a 4-7 km thick crustal sequence, and a 8-12 km thick mantle sequence (e.g., Nicolas et al., 2000). The ophiolitic sequence displays a Penrose pseudostratigraphy composed from top to bottom of a sedimentary cover (radiolarian cherts), volcanics (pillow lavas and lava flows), sheeted dykes, isotropic and layered gabbros, peridotites (harzurgites and dunites), and a 300-500 m thick metamorphic sole with an inverted metamorphic grading (e.g., Cowan et al., 2014; Hacker, 1991; Nicolas et al., 2000; Searle and Cox, 1999; Soret et al., 2017). The ophiolite overlies a sequence of deep-marine, Permian to Cretaceous sediments interpreted to be derived from the distal Arabian margin or the adjacent oceanic crust – the Hawasina nappes – and underlying Arabian margin-derived nappes (Béchennec et al., 1990).

In the northern part of the ophiolite, the extrusive sequence is geochemically layered (Ernewein et al., 1988; Nicolas et al., 2000). Basalts with a geochemistry

similar to mid-ocean ridge basalts (N-MORB) dominate in the lower part of the volcanic sequence, called *Geotimes Unit* or *Unit V1* by Ernewein et al. (1988). Above this unit are the Lasail and Alley volcanic suites, collectively termed *Unit V2* by Ernewein et al. (1988), which consist of depleted arc tholeiites and boninites interpreted as products of hydrous melting of a previously depleted mantle source (e.g., Godard et al., 2006). This geochemical pattern in the crustal sequence of the Oman ophiolite led to the formulation of different tectono-magmatic models invoking formation either in an open ocean (e.g., Nicolas, 1989) or above an active subduction zone (e.g., Pearce et al., 1984). A more recent study, however, suggested that the Geotimes MORBs may have been produced under high water content, hence more likely above an incipient subduction zone (MacLeod et al., 2013).

Paleomagnetic data from the extrusive sequence of the Semail ophiolite indicate a rigid block clockwise (CW) rotation up to ~150° in the northwestern segment of the ophiolite (north of the Hawasina tectonic window), and only minor counterclockwise (CCW) rotations up to ~20° in the southeastern portion of the ophiolite (Feinberg et al., 1999; Perrin et al., 2000; Weiler, 2000). This was originally interpreted as the result of major relative rotations between the northern and southern part of the ophiolite (Nicolas et al., 2000; Perrin et al., 2000), until Feinberg et al. (1999) and Morris et al. (2016) documented the occurrence of a pervasive remagnetization of the ophiolite in the southern segment, which occurred during or soon after the Late Cretaceous emplacement of the ophiolite above the Arabian continental margin (e.g., Nicolas et al., 2000; Searle and Cox, 1999; Searle et

al., 2004). In particular, Morris et al. (2016) suggested that the minor CCW rotation of the southern block occurred after the remagnetization event.

Zircon U-Pb dating of the plutonic section of the Semail ophiolite indicates that the ophiolitic crust formed at a fast spreading ridge in less than ~1 Ma in the Late Cretaceous (~96-95 Ma; Rioux et al., 2016), only just preceding other Neo-Tethyan ophiolites from Turkey and Cyprus with 94-90 Ma ages (e.g., Maffione et al., 2017). Zircon U-Pb and hornblende and mica Ar-Ar ages from garnet-bearing metamorphic sole rocks are similar or slightly younger than the magmatic sequence (96.2-92.6 Ma; Hacker et al., 1996; Rioux et al., 2016; Warren et al., 2005), indicating cooling and exhumation of the sole synchronous with upper plate spreading and formation of the ophiolitic crust (e.g., van Hinsbergen et al., 2015). More recently, garnet Lu-Hf ages from the uppermost, garnet-bearing layer of the metamorphic sole in Oman have constrained subduction-related prograde metamorphism at 104 Ma (Guilmette et al., 2018) and a nearly identical Lu/Hf age was reported from Turkey (Pourteau et al., 2018), indicating near-synchronous timing of subduction initiation. According to these new results, upper plate spreading (and ophiolite formation) postdated the initiation of subduction by ~8-12 Ma. Because spontaneous subduction initiation requires initial slab roll-back and simultaneous upper plate extension (Stern et al., 2012), this delay demonstrates that subduction initiation must have been induced (Guilmette et al., 2018), i.e. triggered by a far-field tectonic stress.

3. Sampling and methods

A total of 380 standard paleomagnetic samples were collected from 12 localities within the sheeted dyke section (10 sites) and the extrusive sequence (2 sites) (Figure 1). All samples were drilled in the field using a water-cooled portable rock drill, and were oriented in situ using both magnetic and sun compasses. Mean paleomagnetic directions for each sampling site were calculated by averaging characteristic remanent magnetizations (ChRMs) interpreted from typically 20-50 samples collected from six to eleven adjacent chilled margin-bearing dykes. Orientation of the volcanic sequence at two sites was determined using the primary layering of pillow lavas and an intercalated lava flow unit.

The nature of the magnetic carriers was characterized through rock magnetic experiments and thin section analysis carried out at the paleomagnetic laboratory 'Fort Hoofddijk' at Utrecht University (Netherlands). High-temperature thermal variation of the magnetic susceptibility was investigated via heating-cooling cycles from room temperature to 700°C in argon atmosphere using a KLY-3 Kappabridge (AGICO) coupled with a CS3 apparatus. The Curie temperatures were determined from the thermal demagnetization results. Hysteresis parameters were calculated through hysteresis loops with peak fields of 0.6-1.5 T, using an alternating gradient magnetometer (Micromag AGM, Princeton). Mineralogical assemblages and the nature and distribution of the ferromagnetic minerals were determined by analizing polished thin sections under both transmitted light and scanning electron microscope (JEOL JCM-6000), and by carrying out elemental analysis with an energy-dispersive X-ray (EDX) analyzer coupled with the SEM.

Remanence components were analyzed using mainly stepwise alternating field (AF) demagnetization with variable increment steps from 5 to 100 mT. About 10% of the samples were also demagnetized thermally in a magnetically shielded furnace (ASC, TD48-SC) using variable increment steps from 100° to 580°C (or until complete demagnetization). AF demagnetization and measurement of the remanence after each demagnetization step were conducted using a robotized superconducting (SQUID) cryogenic magnetometer (Mullender et al., 2016) located in a magnetically shielded room. Demagnetization data were plotted on orthogonal diagrams (Zijderveld, 1967) and the remanence components were isolated via standard principal component analysis (Kirschvink, 1980) using the online software package www.paleomagnetism.org (Koymans et al., 2016). ChRM components with maximum angular deviation (MAD) larger than 10° were discarded from further analysis. Site mean ChRM directions were computed using Fisherian statistics (Fisher, 1953) on virtual geomagnetic poles (VGPs) associated to the isolated ChRMs, and after having applied a fixed 45° cutoff to the VGPs.

The computed site mean directions were then used to calculate the tectonic rotations at each site using a net tectonic rotation approach (Allerton and Vine, 1987). This technique prevents possible biases associated with classic tilt correction in units lacking paleohorizontal constraints, like sheeted dykes, and has been successfully applied to other ophiolites (e.g., Maffione et al., 2017; Morris et al., 1998). Rather than decomposing the deformation into a tilt and a vertical axis rotation component, a net tectonic rotation analysis computes the single rotation around an inclined axis that restores both the rock unit to its original orientation

(i.e., vertical for sheeted dykes) and the measured *in situ* remanence to a selected reference direction. The reference direction is the direction of the magnetic field at the time and latitude at which the remanence was acquired. The declination of the reference direction is inferred from the geocentric axial dipole (GAD) hypothesis (i.e., the time-averaged declination of the magnetic field points towards the geographic north pole), and is therefore D = 000°. The inclination of the reference direction has been calculated by combining all the existing (not remagnetized) paleomagnetic data from the layered gabbros and the extrusive sequence (Perrin et al., 2000; Shelton, 1984; Weiler, 2000), including the results from the two pillow basalt sites in this study. The tilt corrected mean inclination calculated from this dataset, representing the inclination of the reference direction, is 21.5° ± 6.6° (Figure S1).

A set of net tectonic rotation solutions is expressed as (i) azimuth and plunge of the rotation axis, (ii) magnitude and sense of the rotation, and (iii) initial strike of the unit. When applied to vertical units like dykes, two permissible sets of net tectonic rotation solutions are obtained if the dykes can be restored to the vertical. In this case, three selection criteria are used to choose the preferred solution at each site: (1) the calculated rotation has to restore the units to their current position (e.g., a solution yielding overturned beds when units are just gently dipping should be discarded); (2) both the rotation sense and magnitude have to be consistent with the known regional and/or local deformation pattern; (3) multiple sites within a relatively small area have to show similar net tectonic rotation parameters (assuming local rotations are minor).

One set of solutions is instead obtained when dykes are not restored to vertical (e.g., because they did not intrude vertically). Single solutions are geologically meaningless and should be discarded as both the initial dyke orientation and the rotation parameters will only depend on the orientation of the reference direction (e.g., the initial dyke orientation will always strike perpendicular to the reference direction, hence will always be E-W).

Once a preferred solution has been chosen, an iterative net tectonic rotation analysis (Morris et al., 1998; Koymans et al., 2016) is then used to model the uncertainties on the reference direction (only its inclination), the site mean direction, and the dyke orientation. This routine within the net tectonic rotation analysis package is available at www.paleomagnetism.org and produces at each site 75 permissible solutions per set of solutions (hence 150 when dykes are restored to vertical).

4. Results

4.1 Magnetic carrier analysis

Temperature variation of the magnetic susceptibility (Figure 2) is irreversible, with susceptibility values being commonly lower after heating, hence showing mineralogical transformations induced by the experiments. These transformations did not produce new mineralogical phases, as the Curie temperatures for the heating and cooling curve are the same. On the other hand, in the pillow lavas (site

MA01; Figure 2) variable Curie temperatures are inferred from the heating and cooling paths. Curie temperatures of 570-580°C are observed within the dyke samples (Figure 2), indicating nearly pure magnetite as magnetic carrier (Dunlop and Özdemir, 1997). Sites DA and HA show additional Curie temperatures between 300° and 330° (Figure 2), which is consistent with a minor occurrence of iron sulphides, likely pyrrhotite. If present, the break-down of iron sulphides expected during heating at ~500°C (Dunlop and Özdemir, 1997) did not produce any new magnetite as our experiments were conducted in argon atmosphere, hence in reducing conditions. This would explain the lower susceptibility values of the cooling curves in all sites (except site AS where new magnetite might indeed have formed during the experiment; Figure 2). The removal of iron sulphides during the heating is further supported by the absence of inflections in the cooling paths around 300-330° (Figure 2). Site AS shows a slightly higher Curie temperature of 595°C, suggesting the occurrence of partly oxidized (maghemitized) magnetite, common in mafic magmatic rocks (Dunlop and Özdemir, 1997). Pillow lavas from site MA01 show two Curie temperatures of ~545°C and ~450°C, compatible with the occurrence of both Ti-poor and Ti-rich titanomagnetite, respectively. Similar blocking temperatures have also been observed at all sites during the thermal demagnetization experiments, confirming the occurrence of magnetite, titanomagnetite, and (titano)maghemite as main carriers of the magnetization in the samples dykes and lavas.

Relatively narrow to more open hysteresis loops characterize all the dyke samples (Figure 3), indicating the predominance of pseudo-single-domain (PSD;

0.05-3 μm) and perhaps minor single-domain (SD; < 0.05 μm) grains (Dunlop and Özdemir, 1997). On the other hand, pillow lava samples show very narrow hysteresis loops (Figure 3), which are typically observed in rocks dominated by multidomain (MD; >3 μm) ferromagnetic grains (Dunlop and Özdemir, 1997).

Ten thin sections from both dykes and pillow lavas were analyzed. The main mineralogical assemblage in dykes is, in order of abundance, plagioclase, clinopyroxene, orthopyroxene, chlorite, and opaque minerals. In some dyke samples (sites AA and HU) opaque minerals are as large as 0.1-0.2 mm. Pillow lavas are much more weathered and altered than the dykes. The microscopic fabric of both dykes and pillow lavas is purely magmatic, with frequent euhedral plagioclase and pyroxene minerals (more commonly observed in dykes) forming a matrix with no internal fabric. The opaque minerals are also randomly dispersed within this matrix. Chlorite, which is always present in all the samples, occurs randomly dispersed within the isotropic matrix, suggesting a static metamorphism likely associated to seafloor hydrothermal alteration, as frequently observed in other ophiolites (e.g., Maffione et al., 2017). Such metamorphism occurs at very low temperatures and normally does not affect the magnetic remanence of rocks emplaced at a mid-ocean ridge.

SEM analysis and EDX characterization (Figure 4), revealed the occurrence of angular magnetite and titanomagnetite, sometimes with exolution lamellae, with grain sizes variable between 1 μm (pseudo-single-domain – PSD) and 100 μm (multidomain – MD). At few samples from sites FF and AS, iron- and titanium-rich oxides up to 1 mm in size and showing compositional bands have been observed

and interpreted as ilmenite. This is supported by the fact that the magnetization of samples carrying such large ilmenite minerals (which is not magnetic) is comparable to that of other samples.

4.2 Paleomagnetic results

Natural remanent magnetization (NRM) intensity from 380 analyzed samples varies between several 10s of mA/m and 4 A/m, suggesting substantial variations in ferromagnetic mineral concentration across the sampled rocks. A total of 340 characteristic remanent magnetizations (ChRMs) were interpreted from the 380 analyzed samples, with the remaining 40 samples showing noisy, uninterpretable demagnetization diagrams, or MAD values above the chosen threshold of 10°.

AF demagnetization diagrams show two components of magnetization: a low-coercivity viscous component usually removed at 10-15 mT, and a stable high-coercivity component isolated within an interval between 20 and 100 mT (Figure 5). At about half of the samples, these high-coercivity components were isolated using great circle fitting (McFadden and McElhinny, 1988), which denoted the occurrence of high-coercivity phases that could not be removed at 100 mT. We suspect this effect might be associated with partial maghemitization of the original magnetite, which causes a slight increase of coercivity. Although this hypothesis remains a valid explanation for the remanence behavior, is not supported by thin section microscope analyses. This might be due to the fact that cracks associated with maghemitization of original (titano)magnetite can sometimes be difficult to identify in thin section.

Overall, AF demagnetization treatment was more effective in isolating the ChRM components (Figure 5), and produced more stable demagnetization components compared to the thermal demagnetization technique (Figure 5E). Nevertheless, the ChRM directions determined from both AF and thermally demagnetized twin specimens are fully consistent (Figure 5C), showing that these are high-stability, likely primary remanence components suitable for tectonic interpretations.

Site mean directions (*in situ* coordinates) at 10 out of 12 sites (Figure 6; Table 1) are significantly different from the present-day GAD field direction at the mean latitude of the Oman ophiolite (D/I = 000°/42°), hence ruling out any recent remagnetization. The remaining two sites (AA and MU) show northerly mean directions that are very close to the expected inclination of the present-day GAD, suggesting possible recent remagnetization (Figure 6; Table 1). For now, this remagnetization cannot be confirmed based on this evidence alone and therefore we use all sites for the net tectonic rotation analysis. At site HU, several ChRM directions that are close to the present-day GAD direction were discarded due to possible recent remagnetization before computing the site mean direction.

Besides sites AA and MU with northerly directions, the other ten sites show *in situ* site mean directions varying between southeastward, northeastward, and northwestward directions (Figure 6; Table 1). The tilt-corrected mean direction from the two combined pillow lava sites (MA01 and MA02) has D = 093.4° and I = 15.9°, and indicates a vertical axis rotation of 93.4° CW (Table 1). This is consistent with previous results (Morris et al., 2016; Perrin et al., 2000) indicating large CW

rotation of the whole ophiolite, and provides a first-order approximation for the vertical axis rotation component expected at the other dyke sites.

Fold tests to check the primary nature of the interpreted ChRMs cannot be performed in units lacking paleohorizontal control such as dykes. Similarly, fold tests could not be performed on the two pillow lava sites, as rocks there are part of the same outcrop and have the same orientation. In this case VGP distribution may be used to assess the primary nature of the remanence based on the criteria suggested by Deenen et al. (2011). VGP scatters at all the sites except HA and is consistent with the expected scatter induced by paleosecular variation (A_{95min}<A_{95}<A_{95max}; Figure 6 and Table 1). The scatter of ChRMs at site HA is smaller than that produced by secular variation (i.e., A_{95} < A_{95min}; Table 1), yet, this may be explained by the fact that the majority of the remanence directions (i.e., 18 out of 30) at this site have been computed using great circles analysis (McFadden and McElhinny, 1988). Although mathematically and statistically reliable, these directions do not necessarily replicate the natural scatter of the directions due to secular variation of the geomagnetic field. Therefore, based on the above evidence and in the absence of other constraints to assess the nature of the remanence, we assume for now that the remanence at all sites could be primary.

4.3 Net Tectonic Rotation analysis

Net tectonic rotation analysis of the ten sheeted dyke sites succeeded in restoring both the dykes back to their original (vertical) orientation and the

computed in situ paleomagnetic directions to the chosen reference direction, generating two sets of permissible solutions at each site (Table 2). Because the Oman ophiolite underwent an overall large (up to 150°) CW vertical axis rotation (see Morris et al. (2016) for a comprehensive review), preferred solutions were selected among those satisfying all the three criteria listed in the Methods section. Based on these criteria, site BB was discarded as both solutions indicated large CCW rotations, which are at odds with the regional CW rotation of the ophiolite. This might be explained by the fact that the primary remanence at site BB has been overprinted, hence giving meaningless net tectonic rotation solutions. This hypothesis is supported by the fact that site BB is within the southern domain of the Oman ophiolite that has been affected by remagnetization during the obduction stage (Morris et al., 2016).

Net tectonic rotation analysis at site MU provided two solutions, one of which is clearly meaningless for it gives extremely large CCW rotations. The other set of solutions indicates a CW rotation but the vertical-axis component of this net rotation is quite small and therefore not consistent with the regional large rotation of the ophiolite. Because the in situ remanence of site MU is close to the present-day field (Table 1 and Figure 6), it is indeed likely that this site has been (totally or partially) affected by recent remagnetization. We therefore will not consider the result from this site for further analysis.

Net tectonic rotation analysis at site AA provided two solutions, one producing a CCW rotation (hence discarded) and the other a CW rotation that is potentially consistent with the regional deformation pattern. The rotation pole for

this potential preferred solution is between and similar, within error, to both the reference direction and the site mean remanence direction (Table 2). As pointed out by Allerton and Vine (1987), in this circumstance the error associated with the calculation of the net tectonic rotation parameters might be very high. Although all the parameters for this (potentially) preferred solution are consistent with the other sites, we prefer to adopt a conservative approach and discard this site from further analysis.

Preferred solutions could instead be selected at the remaining seven sites (Table 2). In particular, at sites AS, HA, and GD the preferred solutions are those giving CW rotations (while the alternate solutions provided CCW rotastions). The net tectonic rotation analysis for the remaining four sites DA, FF, HD, and HU yielded CW rotations at both sets of solutions. At sites FF, HD, and HU, the preferred solutions have been selected among those giving the largest vertical-axis rotation (the alternative solutions have shallower axes and smaller net rotations that result in minimum vertical axis rotations, which are incompatible with the large rotation observed regionally). Both solutions at the remaining site DA produce an equal amount of vertical axis rotation, yet the alternate (i.e., rejected) solution together with vertical axis rotation produces overturned units, which is not compatible with the overall gentle tilt of the ophiolite (Nicolas et al., 2000).

For these seven preferred solutions we have then modeled the uncertainties associated with the mean paleomagnetic direction, the dyke orientation, and the reference direction (Figure 7; Table 2). The rotation axes at these seven sites are moderately to steeply plunging approximately to the west (sites AS, FF, and GD), to

the north-northeast (sites HA, HU, and HD), and to the southeast (site DA). The rotation magnitude is variable between ~80° and ~160°, consistent with the large regional rotation of the ophiolite (Morris et al., 2016). There seems to be no correlation between the orientation of the rotation axes or the magnitude of the net rotations and the location of these seven sites.

The calculated initial dyke strike is consistently NNE to ENE (Table 2 and Figure 7). When the modeled initial dyke orientations from all seven sites are plotted together (525 directions), the most frequent initial strike of the sheeted dykes at the scale of the whole ophiolite is NNE-SSW, between 020° and 030° (Figure 7). A bimodal distribution seems to appear in this diagram, with primary NNE-SSW and secondary ENE-WSW directions. We consider the predominant (more frequent) NNE-SSW trend as representative of the direction of the spreading ridge at which these dykes were emplaced in the Cretaceous. The ENE-WSW directions, if meaningful, may be related to dykes locally intruded at an angle to the NNE-SSW trending spreading ridge, or to an artifact of the modeling.

5. Discussion

Our results indicate that the oceanic crust of the Oman ophiolite accreted at a NNE-SSW trending spreading center, which, given the geochemical and geochronological evidence was located in the upper plate above an infant subduction zone (Guilmette et al., 2018; MacLeod et al., 2013; Rioux et al., 2016). Interestingly, regardless of the geochemical signature of the ophiolitic crust, the

orientation of this spreading center already makes it quite unlikely that the crust of the Oman ophiolite formed at the Neotethyan mid-oceanic ridge as suggested before (e.g., Nicolas et al., 2000): the overall strike of the Gondwana passive margins, and hence of the Neotethys ridge, was NW-SE rather then ~NNE-SSW (in Cretaceous paleomagnetic coordinates) (Figure 8b).

The location, in present-day coordinates, of the subduction zone above which the Oman ophiolite was formed is best estimated from the modern obduction front in the western and southern edge of the ophiolite, although post-obduction erosion may have removed some of the most trench-proximal parts of the ophiolite. The sheeted dyke sections strike approximately sub-parallel to this obduction front, suggesting that the spreading occurred orthogonal to the trench. This is further suggested by the narrow, 96-95 Ma age range of the ophiolitic crust along the ophiolite's strike (Rioux et al., 2016). Such a narrow age range is expected when a fast-spreading ridge is located parallel to the subduction front. Upon spreading, this supra-subduction zone ridge migrates away from the trench at half-spreading rate. With spreading rates of 5-10 cm/yr estimated for the Semail ophiolite (Rioux et al., 2016), and an exposed width orthogonal to the obduction front of <100 km, only 1-2 Myr worth of ophiolite spreading history can be preserved in the modern ophiolite, whereas all crust that accreted due to younger spreading must be located offshore northern Oman (Figure 8d). Had spreading occurred parallel to the trench, the 500 km long ophiolite should have had crustal ages spanning 5-10 Myr from north to south (Maffione et al., 2017). We therefore conclude that the subduction zone above

which the Oman ophiolite accreted was also striking NNE-SSW, parallel to the restored dyke orientation.

A NNE-SSW original orientation of the ophiolite is fully consistent with the vertical axis rotations estimated from paleomagnetic data (Morris et al., 2016) suggesting that the ophiolite underwent up to ~150° clockwise rotation between the formation of its crust at ~96-95 Ma, and the end of obduction around 70 Ma (Morris et al., 2016). Back-rotating the ophiolite around its modern northwestern tip to its original NNE-SSW strike provides the minimum horizontal displacement between subduction initiation and obduction. Such a rotation, along a small circle at the ophiolite's southeastern tip, involves a total horizontal motion relative to Arabia of ~1000 km. This gives an average long-term drift rate of ~4 cm/yr, which is well within the ranges of similar strongly rotating trenches that roll back along and obduct passive margins (e.g., Chertova et al., 2014). This restoration places the ophiolite's northern (i.e. modern eastern) tip at a paleolatitude of ~5°N. Paleolatitudes calculated from the ophiolite's crust allow for a somewhat more northerly paleolatitude for ophiolite spreading, and the plate motion rates during ophiolite-Arabia convergence may thus have been somewhat higher. Nevertheless, this analysis shows that the ultra-high spreading rates inferred based on U/Pb crustal ages (Rioux et al., 2016) must have been short-lived, focused in the period of inception of upper plate spreading.

Perrin et al. (2000) showed rapid clockwise rotations during ophiolite formation, from major declination differences within the effusive sequence. Whilst the rotation sense and magnitude of these rotations are consistent with the total

rotation of the whole ophiolite, the short time span during which the effusive rocks accumulated of only a few million years makes it unlikely that these rotations represent the rotation of the entire ophiolite: if they were representative, these would require plate motion and subduction rates of up to meters per year, which is geodynamically unrealistic. We therefore infer that the results reported in Perrin et al. (2000) reflect tectonic deformation within the ophiolite, e.g. along transform faults, which may cause local rotation, as observed in the Troodos ophiolite of Cyprus (Morris and Maffione, 2016).

Our reconstructed initial trench orientation associated with the Semail ophiolite now allows assessing the nature of the weakness zone at which subduction initiated – the main aim of our study. A NNE-SSW original strike of the subduction zone is approximately orthogonal to the Arabian passive continental margin at ~95 Ma, when corrected for plate motions in a paleomagnetic reference frame (Torsvik et al., 2012). Weakness zones expected in such an orientation are likely to be fracture zones. This conclusion for the Semail ophiolite does not come in isolation: coeval ophiolites from Cyprus, Syria, and Turkey all share a similar ridge and inferred trench orientation, and also in those settings, trenches and supra-subduction zone ridges were striking N-S to NE-SW, orthogonally to restored passive margins (Maffione et al., 2017) (Figure 8b). Moreover, such a former fracture zone orientation is preserved in the Arabian margin today along the N-S striking coast of northern Oman and the UAE, connecting passive margins of northeast Oman, and the restored margin of the Zagros mountains in Iran (Figure 8b). It thus appears that Cretaceous subduction initiation in the Neotethys Ocean

was driven by (ES)E-(WN)W contraction, rather than the widely inferred ~N-S convergence. This may help in our search for the potential drivers of subduction initiation.

When the underthrusting of the Arabian passive margin at the Zagros collision zone of Iran is restored (McQuarrie and van Hinsbergen, 2013), the original Oman-UAE fracture zone margin, of Permian age (Béchennec et al., 1990; Stampfli and Borel, 2002), extended several hundreds of kilometers farther to the north than today (Figure 8b). We restore the original orientation of the ophiolite, and of the newly formed subduction zone at which the ophiolite's sole started forming just before 104 Ma, adjacent to this ancient Arabian continent-parallel fracture zone. The initiation probably occurred sufficiently far east of the margin to be in an intra-oceanic setting, since no continental crust relics are found in the ophiolite, but nevertheless close to that continental margin.

Near-continental margin intra-oceanic subduction initiation and formation of supra-subduction zone ophiolites was restored for the Indus-Yarlung ophiolites of southern Tibet (Maffione et al., 2015b). There, it was thus already inferred that supra-subduction zone ophiolites are not necessarily associated with subduction initiation in the vicinity of a mid-ocean ridge. In this study, we propose a similar scenario for the Semail ophiolite, where mid-ocean ridge inversion has long been the preferred model (Boudier et al., 1988; Duretz et al., 2016). Our reconstruction places Arabian lithosphere in the upper plate, but even if subduction initiated farther to the northeast such that oceanic crust adjacent to the Zagros margin was located in the upper plate, it is quite unlikely that an active ridge was present there

at that time. Active mid-ocean ridges are commonly not observed in the vicinity of a 170 Myr old passive margin, and as pointed out by Maffione et al. (2017), it is unlikely that the Cretaceous Neotethys ocean between Arabia and Eurasia still contained an active mid-ocean ridge: the ridge at which the Neotethys opened would have long subducted below the Iranian active margin by that time (such as inferred by Stampfli and Borel (2002)). We may thus infer that, in absence of an active mid-ocean ridge in an ocean, passive margins, or fracture zone margins, may be the preferred locus of subduction initiation.

Such settings of continental margin-parallel fracture zones are today abundant along the west and east coast of Africa (Figure 8a). Recent studies have shown through seismic interpretation that the fracture zone margin of west Africa was associated with hyperextension and exhumation of serpentinized mantle during continental breakup (Gillard et al., 2017). Serpentine-rich faults along hyperextended margins are weak and may localize subduction initiation upon forced convergence (Maffione et al., 2015a). We envisage that such a setting may have facilitated subduction initiation in the Oman case, although we note that the old age of this setting at the time of subduction initiation (~170 Myr) renders it likely that a thick, unbroken lithospheric mantle was present, whose strength must be overcome to initiate subduction.

Our results, and those of Maffione et al. (2017) for the Mediterranean region, raise several first-order new questions for understanding subduction initiation dynamics. Our results show that Cretaceous subduction initiation within the Neotethys ocean formed a new plate (the Anadolu plate of Gürer et al. (2016)

separated from Eurasia and Africa-Arabia by trenches (Figure 8). This plate must have moved westward relative to Africa/Arabia (and Eurasia, given overall N-S Africa-Eurasia convergence) to drive subduction initiation along N-S striking trenches. Gaina et al. (2015) showed based on Indian Ocean reconstructions that prior to the end of the Cretaceous superchron, India rotated counterclockwise relative to Arabia that requires such convergence. Did the driver of this rotation also spark subduction initiation farther westwards? And what processes cause the hot conditions recorded in the Oman metamorphic sole 8 Myr of upper plate spreading (Guilmette et al., 2018) with subduction initiating in old, cold lithosphere? We refrain from speculating on these questions, but leave these for future study and debate.

6. Conclusions

The subduction zone above which the crust of the Semail ophiolite of Oman formed is widely thought to have initiated along, or in the vicinity of a Neotethyan mid-oceanic ridge. In this paper, we restored the paleo-orientation of the supra-subduction zone ridge at which the Semail ophiolitic crust accreted around ~96-95 Ma, through paleomagnetic analysis of its sheeted dyke sections. Our results from seven localities covering the entire width of the ophiolite consistently show that this ridge was orientated NNE-SSW. We infer that the trench orientation, marked by the modern obduction front, was oriented sub-parallel to this trench. Our results thus indicate that the trench orientation was approximately orthogonal to the Arabian

passive margin. We infer that subduction initiated along a fracture zone that was located parallel to, and likely in the vicinity of, the fracture zone that connected the Permian Arabian passive margin of northern Oman with the margin underthrust below Iran at the Zagros collision zone. This places Arabian continental crust in the upper plate during subduction initiation. Subduction hence did not initiate in the vicinity of the Neotethyan ridge, which according to plate reconstructions had long been subducted during Cretaceous subduction initiation. We conclude that subduction was induced by (ES)E-(WN)W contraction, as previously also inferred for ophiolite belts of the eastern Mediterranean and NW Arabian margins. This may help the future identification of the dynamic trigger of subduction initiation in the Neotethys Ocean.

Acknowledgements

DJJvH acknowledges a Netherlands Organization for Scientific Research (NWO) VIDI grant 864.11.004. CG acknowledges a NSERC-DG grant #RGPIN-2014-05681. We thank Benoit Charette for field assistance.

Figure Captions

Figure 1. Geological map of the Oman ophiolite.

Figure 2. High-temperature variations of low-field magnetic susceptibility (k) for six representative samples (five from dykes and one from pillow lavas). Diagrams are mainly irreversible, showing mineralogical transformation during heating. Curie temperatures have been inferred from the heating paths.

Figure 3: Hysteresis loops for six representative samples (the same as in Figure 2), showing predominantly narrow to slightly open loops typical of multidomain (MD) magnetic grains.

Figure 4: Back-scattered electron (BSE) images of representative thin sections from sheeted dykes showing the presence of iron oxides (magnetite, titanomagnetite, and possibly ilmenite) with variable size from ~1 μm to ~1 mm.

Figure 5: A-F - Representative orthogonal vector plots (Zijderveld diagrams) of both alternating field and thermal demagnetization for various sites (in situ coordinates). C – An example of consistent ChRM directions acquired in AF and TH demagnetized sister samples. NRM = natural remanent magnetization. Steps are shown in °C or mT.

Figure 6. Stereographic projections of the interpreted characteristic remanent magnetization directions (ChRMs) and virtual geomagnetic poles (VGPs) from all sites. The great circles used in the principal component analysis are shown in the left diagrams (dotted curve), together with the direction isolated from these (small black dots). The middle ChRM plots show all the ChRM directions calculated from best-fit lines and great circle analysis (blue dots = normal polarity; open dots = reverse polarity; gray dots = discarded direction after 45° cut-off). The red ellipse is the cone of confidence around the computed mean direction, while the light blue shaded area is the error on the mean declination (ΔD in Table1). The VGP plots on the right of each site show the accepted VGPs (blue dots) and the discarded VGPs (gray dots), which in fact fall outside the solid inner circle that represents the 45° cut-off. The Grey star in the left plots is the present-day GAD field direction.

Figure 7. (Left) Stereographic projections of the permissible initial dyke orientations (rose diagram) and rotation poles calculated after modeling of the uncertainties associated to the input vectors of the net tectonic rotation analysis, following methods of Morris et al. (1998) and Koymans et al. (2016). (Right) Frequency distribution of the permissible rotation magnitude obtained from the same analysis. Summary plots showing the mean initial dyke orientation and rotation magnitude are shown in the bottom right corner, and have been obtained by combining all the permissible results from the seven sites.

Figure 8. Tectonic model of subduction initiation along the Arabian margin of Oman. Reconstruction of continents in paleomagnetic reference frame of Torsvik et al. (2012). Reconstruction of the Zagros margin following McQuarrie and van Hinsbergen (2013), and of eastern Mediterranean subduction initiation and obduction following Maffione et al. (2017). A) Fracture zone and passive margins of the modern African continent, providing a modern example of the restored Arabian-Greater Adria continental margin, where the fracture zone margins were the locus of Cretaceous subduction initiation. Basic plate kinematics requires that the N-S subduction segments were connected with a transform fault parallel to (and here dotted along) the Arabian passive margin. B-D) Subduction initiation parallel and close to the Oman-UAE fracture zone margin around 105 Ma is followed by forearc extension around 96-95 Ma, and subsequent rotation of the forearc Oman ophiolite, followed by ~70 Ma obduction. Bey = Bey Dağları Platform; Kir = Kırşehir Massif, Tav = Tavşanlı Zone; for the tectonic history of the eastern Mediterranean region, see Gürer et al. (2016) and Maffione et al. (2017).

Table 1: *Remagnetized sites. [A] In situ directions. [B] Tilt corrected directions. Lithologies are sheeted dykes (SD) and pillow lavas (PL). δDipDir is the 95% confidence around the mean pole to dyke measured in the field. (N meas.) is the number of dykes measured in the field to calculate the mean direction. ChRM interpretation has used best-fit lines (L) and great circles (GC) fitting. n/N is the number of specimens used in the statistics over the total number of analysed samples. D, dDx, I, dIx are declination and associated error, and inclination and

associated error. α_{95} = semiangle of the 95% cone of confidence around the site-mean ChRM direction (Fisher, 1953). K is Fisher's precision parameter relative to the ChRMs (Fisher, 1953). A_{95} is the semiangle of the 95% cone of confidence around the mean virtual geomagnetic pole (VGP). K is Fisher's precision parameter relative to the VGPs. A_{95min} and A_{95max} are the minimum and maximum semiangle of the 95% cone of confidence expected for the given dataset by paleosecular variation.

Table 2: Results of the net tectonic rotation analysis (Allerton and Vine, 1987) showing the calculated values for the azimuth and plunge of the rotation axis, rotation magnitude and sense, and restored dyke strike and plunge. Reference direction used: D = 000°, I = 21.5° ± 6.6°. In situ dyke orientations and associated uncertainties used for the analysis are in Table 1. Two sets of solutions have been obtained at each site and identified as "preferred" (the one used for the tectonic interpretation) and "alternate" (the one discarded).

Supplementary files: Data (.dir) and statistical interpretation (.pmag) files of the paleomagnetic data that lie at the basis of this paper. Data can be viewed and analyzed at www.paleomagnetism.org (Koymans et al., 2016).

7. References

Agard, P., Jolivet, L., Vrielynck, B., Burov, E., Monié, P., 2007. Plate acceleration: The obduction trigger? Earth and Planetary Science Letters 258, 428-441.

Agard, P., Yamato, P., Soret, M., Prigent, C., Guillot, S., Plunder, A., Dubacq, B., Chauvet, A., Monié, P., 2016. Plate interface rheological switches during subduction infancy: Control on slab penetration and metamorphic sole formation. Earth and Planetary Science Letters 451, 208-220.

Allerton, S., Vine, F., 1987. Spreading structure of the Troodos ophiolite, Cyprus: Some paleomagnetic constraints. Geology 15, 593-597.

Béchennec, F., Le Métour, J., Rabu, D., Bourdillon-de-Grissac, C., De Wever, P., Beurrier, M.t., Villey, M., 1990. The Hawasina Nappes: stratigraphy, palaeogeography and structural evolution of a fragment of the south-Tethyan passive continental margin. Geological Society, London, Special Publications 49, 213-223.

Boudier, F., Ceuleneer, G., Nicolas, A., 1988. Shear zones, thrusts and related magmatism in the Oman ophiolite: initiation of thrusting on an oceanic ridge. Tectonophysics 151, 275-296.

Chertova, M.V., Spakman, W., Geenen, T., van den Berg, A.P., and van Hinsbergen, D.J.J., 2014. Underpinning tectonic reconstructions of the western Mediterranean region with dynamic slab evolution from 3-D numerical modeling. Journal of Geophysical Research 119, 5876-5902.

Cowan, R.J., Searle, M.P., Waters, D.J., 2014. Structure of the metamorphic sole to the Oman Ophiolite, Sumeini Window and Wadi Tayyin: implications for ophiolite obduction processes. Geological Society, London, Special Publications 392, 155-175.

Deenen, M.H.L., Langereis, C.G., van Hinsbergen, D.J.J., Biggin, A.J., 2011. Geomagnetic secular variation and the statistics of palaeomagnetic directions. Geophysical Journal International 186, 509-520.

Dunlop, D.J., Özdemir, Ö., 1997. Rock magnetism: fundamentals and frontiers. Cambridge university press.

Duretz, T., Agard, P., Yamato, P., Ducassou, C., Burov, E.B., Gerya, T.V., 2016. Thermo-mechanical modeling of the obduction process based on the Oman Ophiolite case. Gondwana Research 32, 1-10.

Ernewein, M., Pflumio, C., Whitechurch, H., 1988. The death of an accretion zone as evidenced by the magmatic history of the Sumail ophiolite (Oman). Tectonophysics 151, 247-274.

Feinberg, H., Horen, H., Michard, A., Saddiqi, O., 1999. Obduction-related remagnetization at the base of an ophiolite: Paleomagnetism of the Samail nappe lower sequence and of its continental substratum, southeast Oman Mountains. Journal of Geophysical Research: Solid Earth 104, 17703-17714.

Fisher, R., 1953. Dispersion on a sphere. Proceedings of the Royal Society of London. Series A. Mathematical and Physical Sciences 217, 295-305.

Gaina, C., van Hinsbergen, D.J.J., Spakman, W., 2015. Tectonic interactions between India and Arabia since the Jurassic reconstructed from marine geophysics, ophiolite geology, and seismic tomography. Tectonics 34, 875-906.

Gillard, M., Sauter, D., Tugend, J., Tomasi, S., Epin, M.E., Manatschal, G., 2017. Birth of an oceanic spreading center at a magma-poor rift system. Sci Rep 7, 15072.

Godard, M., Bosch, D., Einaudi, F., 2006. A MORB source for low-Ti magmatism in the Semail ophiolite. Chemical Geology 234, 58-78.

Guilmette, C., Smit, M.A., van Hinsbergen, D.J.J., Gürer, D., Corfu, F., Charette, B., Maffione, M., Rabeau, O., Savard, D., 2018. Forced subduction initiation recorded in the sole and crust of the Semail ophiolite, Oman. Nature Geoscience 11, 688-695.

Gürer, D., van Hinsbergen, D.J.J., Matenco, L., Corfu, F., Cascella, A., 2016. Kinematics of a former oceanic plate of the Neotethys revealed by deformation in the Ulukışla basin (Turkey). Tectonics 35, 2385-2416.

Hacker, B., Mosenfelder, J., Gnos, E., 1996. Rapid emplacement of the Oman ophiolite: Thermal and geochronologic constraints. Tectonics 15, 1230-1247.

Hacker, B.R., 1991. The role of deformation in the formation of metamorphic gradients: ridge subduction beneath the Oman ophiolite. Tectonics 10, 455-473.

Hacker, B.R., Gnos, E., 1997. The conundrum of Samail: explaining the metamorphic history. Tectonophysics 279, 215-226.

Hall, C.E., Gurnis, M., Sdrolias, M., Lavier, L.L., Müller, R.D., 2003. Catastrophic initiation of subduction following forced convergence across fracture zones. Earth and Planetary Science Letters 212, 15-30.

Kirschvink, J., 1980. The least-squares line and plane and the analysis of palaeomagnetic data. Geophysical Journal International 62, 699-718.

Koymans, M.R., Langereis, C.G., Pastor-Galán, D., van Hinsbergen, D.J.J., 2016. Paleomagnetism.org: An online multi-platform open source environment for paleomagnetic data analysis. Computers & Geosciences 93, 127-137.

MacLeod, C.J., Johan Lissenberg, C., Bibby, L.E., 2013. "Moist MORB" axial magmatism in the Oman ophiolite: The evidence against a mid-ocean ridge origin. Geology 41, 459-462.

Maffione, M., Thieulot, C., van Hinsbergen, D.J.J., Morris, A., Plümper, O., Spakman, W., 2015a. Dynamics of intraoceanic subduction initiation: 1. Oceanic detachment fault inversion and the formation of supra-subduction zone ophiolites. Geochemistry, Geophysics, Geosystems 16, 1753-1770.

Maffione, M., van Hinsbergen, D.J.J., de Gelder, G.I.N.O., van der Goes, F.C., Morris, A., 2017. Kinematics of Late Cretaceous subduction initiation in the Neo-Tethys Ocean reconstructed from ophiolites of Turkey, Cyprus, and Syria. Journal of Geophysical Research: Solid Earth 122, 3953-3976.

Maffione, M., van Hinsbergen, D.J.J., Koornneef, L.M.T., Guilmette, C., Hodges, K., Borneman, N., Huang, W., Ding, L., Kapp, P., 2015b. Forearc hyperextension dismembered the south Tibetan ophiolites. Geology 43, 475-478.

McFadden, P., McElhinny, M., 1988. The combined analysis of remagnetization circles and direct observations in palaeomagnetism. Earth and Planetary Science Letters 87, 161-172.

McQuarrie, N., van Hinsbergen, D.J.J., 2013. Retrodeforming the Arabia-Eurasia collision zone: Age of collision versus magnitude of continental subduction. Geology 41, 315-318.

Morris, A., Anderson, M.W., Robertson, A.H., 1998. Multiple tectonic rotations and transform tectonism in an intraoceanic suture zone, SW Cyprus. Tectonophysics 299, 229-253.

Morris, A., Maffione, M., 2016. Is the Troodos ophiolite (Cyprus) a complete, transform fault–bounded Neotethyan ridge segment? Geology 44, 199-202.

Morris, A., Meyer, M., Anderson, M.W., MacLeod, C.J., 2016. Clockwise rotation of the entire Oman ophiolite occurred in a suprasubduction zone setting. Geology 44, 1055-1058.

Mullender, T.A.T., Frederichs, T., Hilgenfeldt, C., de Groot, L.V., Fabian, K., Dekkers, M.J., 2016. Automated paleomagnetic and rock magnetic data acquisition with an in-line horizontal "2G" system. Geochemistry, Geophysics, Geosystems 17, 3546-3559.

Nicolas, A., 1989. Structures of ophiolites and dynamics of oceanic lithosphere. Springer Science & Business Media.

Nicolas, A., Boudier, F., Ildefonse, B., Ball, E., 2000. Accretion of Oman and United Arab Emirates ophiolite–discussion of a new structural map. Marine Geophysical Researches 21, 147-180.

Pearce, J.A., Lippard, S.J., Roberts, S., 1984. Characteristics and tectonic significance of supra-subduction zone ophiolites. Geological Society, London, Special Publications 16, 77-94.

Perrin, M., Plenier, G., Dautria, J.-M., Cocuaud, E., Prévot, M., 2000. Rotation of the Semail ophiolite (Oman): additional paleomagnetic data from the volcanic sequence. Marine Geophysical Researches 21, 181-194.

Pourteau, A., Scherer, E.E., Schorn, S., Bast, R., Schmidt, A., Ebert, L., 2018. Thermal evolution of an ancient subduction interface revealed by Lu–Hf garnet geochronology, Halilbağı Complex (Anatolia). Geoscience Frontiers.

Rioux, M., Garber, J., Bauer, A., Bowring, S., Searle, M., Kelemen, P., Hacker, B., 2016. Synchronous formation of the metamorphic sole and igneous crust of the Semail ophiolite: New constraints on the tectonic evolution during ophiolite formation from high-precision U–Pb zircon geochronology. Earth and Planetary Science Letters 451, 185-195.

Searle, M., Cox, J., 1999. Tectonic setting, origin, and obduction of the Oman ophiolite. Geological Society of America Bulletin 111.

Searle, M., Warren, C., Waters, D., Parrish, R., 2004. Structural evolution, metamorphism and restoration of the Arabian continental margin, Saih Hatat region, Oman Mountains. Journal of Structural Geology 26, 451-473.

Shelton, A.W., 1984. Geophysical studies on the northern Oman ophiolite. Open University.

Soret, M., Agard, P., Dubacq, B., Plunder, A., Yamato, P., 2017. Petrological evidence for stepwise accretion of metamorphic soles during subduction infancy (Semail ophiolite, Oman and UAE). Journal of Metamorphic Geology 35, 1051-1080.

Stampfli, G.M., Borel, G., 2002. A plate tectonic model for the Paleozoic and Mesozoic constrained by dynamic plate boundaries and restored synthetic oceanic isochrons. Earth and Planetary Science Letters 196, 17-33.

Stern, R.J., Gerya, T., 2017. Subduction initiation in nature and models: A review. Tectonophysics.

Stern, R.J., Reagan, M., Ishizuka, O., Ohara, Y., Whattam, S., 2012. To understand subduction initiation, study forearc crust: To understand forearc crust, study ophiolites. Lithosphere 4, 469-483.

Torsvik, T.H., Van der Voo, R., Preeden, U., Mac Niocaill, C., Steinberger, B., Doubrovine, P.V., van Hinsbergen, D.J.J., Domeier, M., Gaina, C., Tohver, E., Meert, J.G., McCausland, P.J.A., Cocks, L.R.M., 2012. Phanerozoic polar wander, palaeogeography and dynamics. Earth-Science Reviews 114, 325-368.

van Hinsbergen, D.J.J., Peters, K., Maffione, M., Spakman, W., Guilmette, C., Thieulot, C., Plümper, O., Gürer, D., Brouwer, F.M., Aldanmaz, E., Kaymakcı, N., 2015. Dynamics of intraoceanic subduction initiation: 2. Suprasubduction zone ophiolite formation and metamorphic sole exhumation in context of absolute plate motions. Geochemistry, Geophysics, Geosystems 16, 1771-1785.

Wakabayashi, J., Dilek, Y., 2003. What constitutes 'emplacement' of an ophiolite?: Mechanisms and relationship to subduction initiation and formation of metamorphic soles. Geological Society, London, Special Publications 218, 427-447.

Warren, C.J., Parrish, R.R., Waters, D.J., Searle, M.P., 2005. Dating the geologic history of Oman's Semail ophiolite: insights from U-Pb geochronology. Contributions to Mineralogy and Petrology 150, 403-422.

Weiler, P., 2000. Differential rotations in the Oman ophiolite: paleomagnetic evidence from the southern massifs. Marine Geophysical Researches 21, 195-210.

Zijderveld, J., 1967. AC demagnetization of rocks: analysis of results, Developments in solid earth geophysics. Elsevier, pp. 254-286.

Figure

Click here to download Figure: Figure_1_Geological_Map_small.pdf

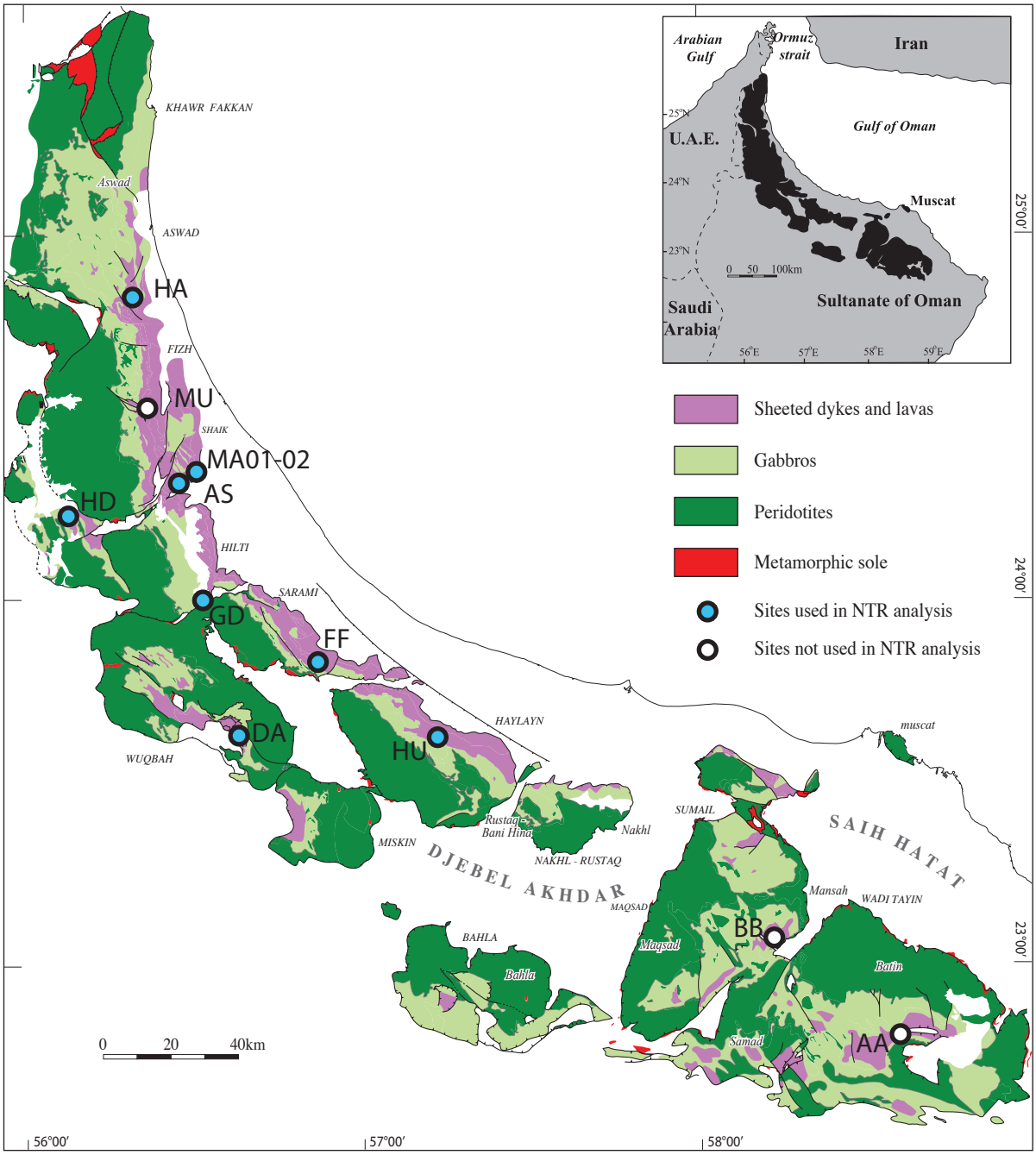

Figure

Click here to download Figure: Figure_2_Thermomag_small.pdf

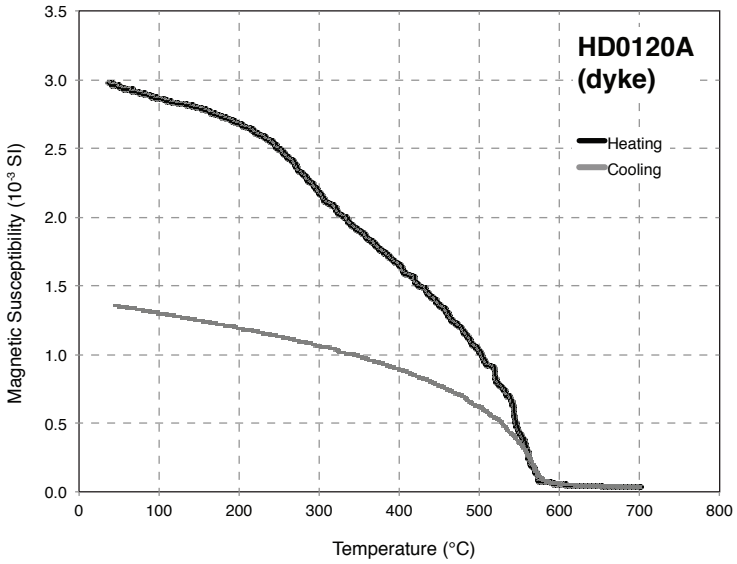

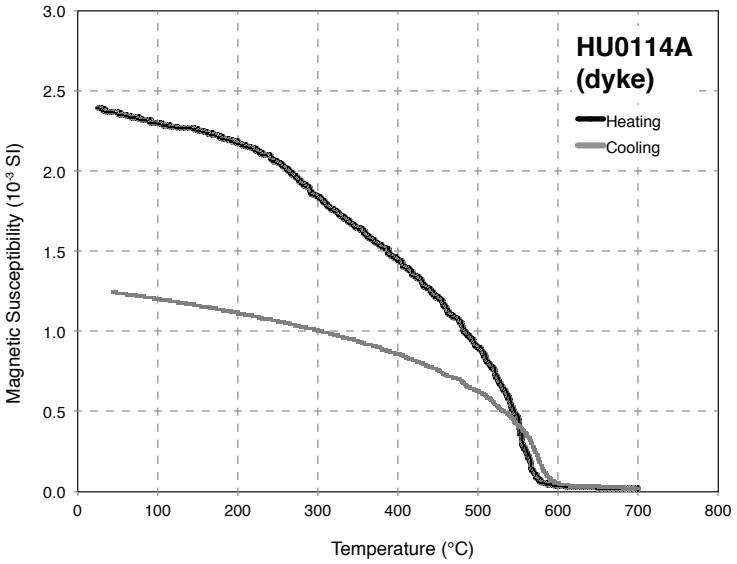

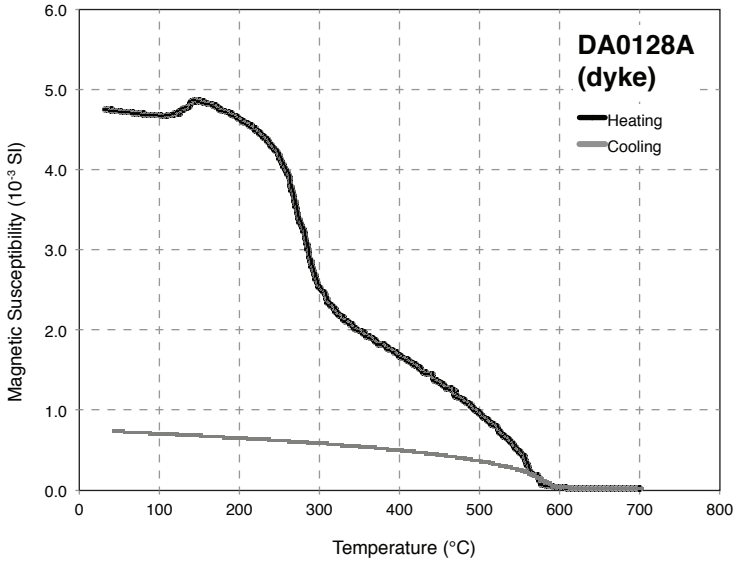

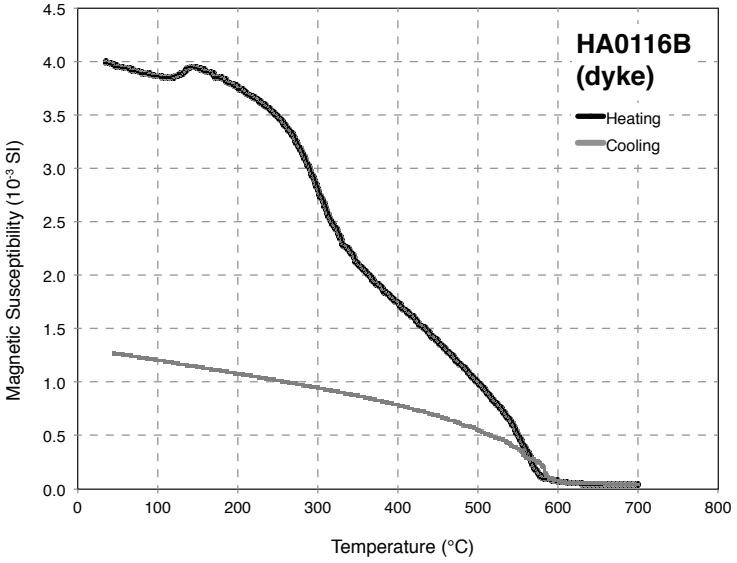

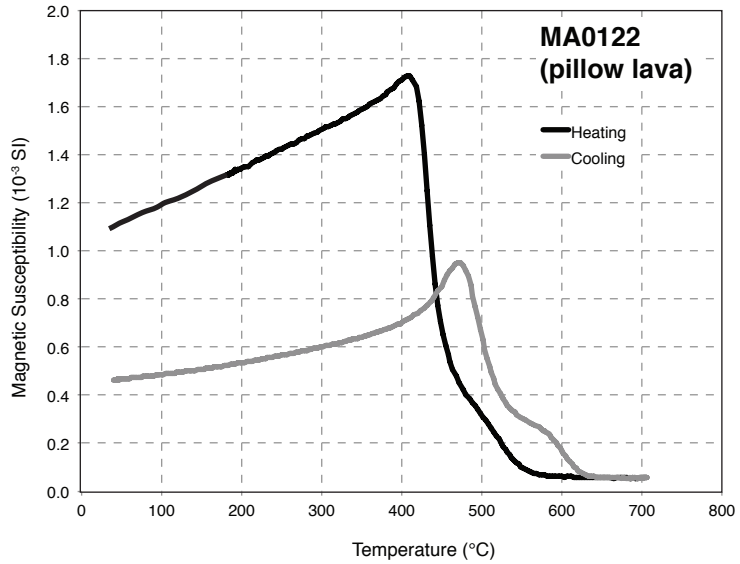

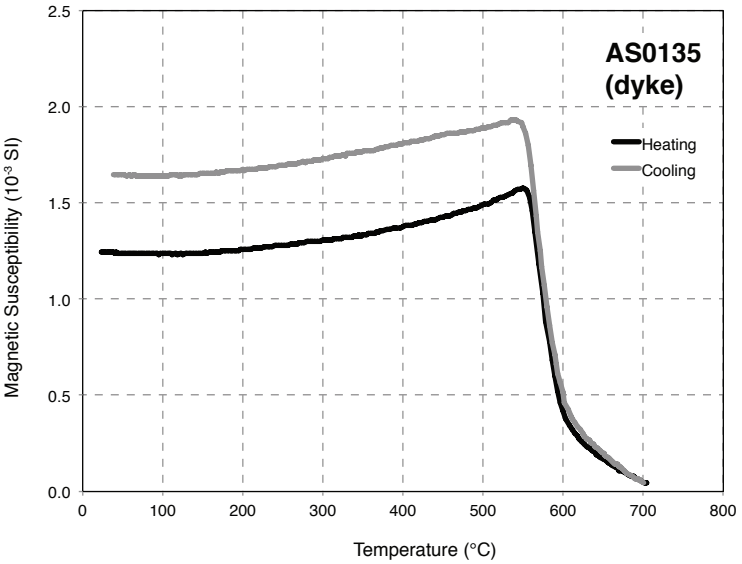

Figure 3

Click here to download Figure: Figure_3_Hysteresis.pdf

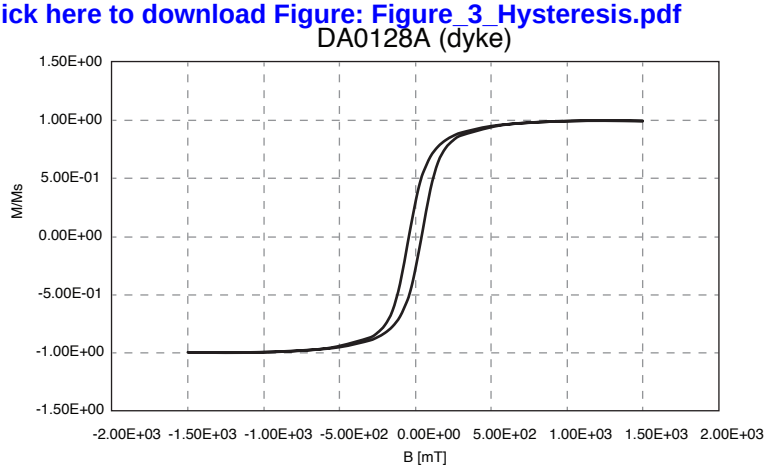

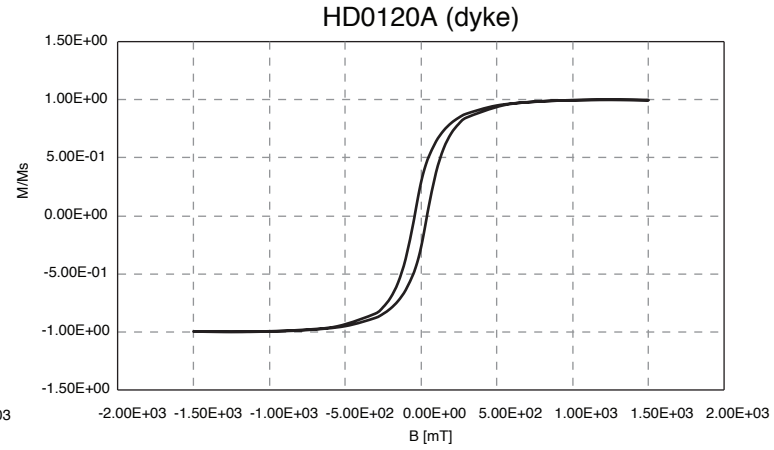

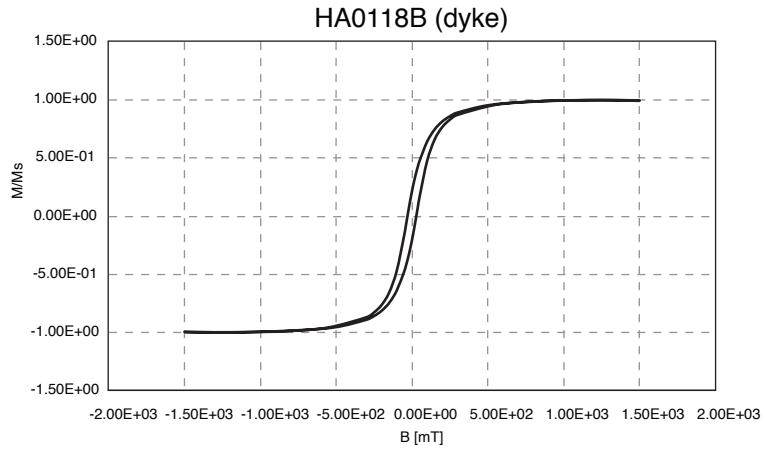

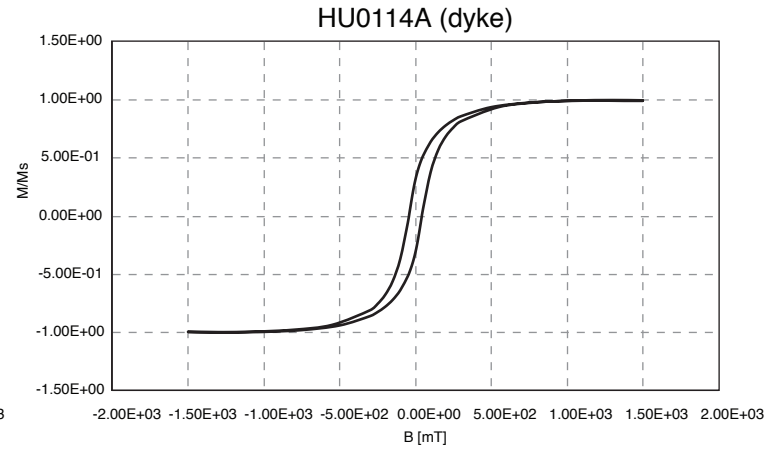

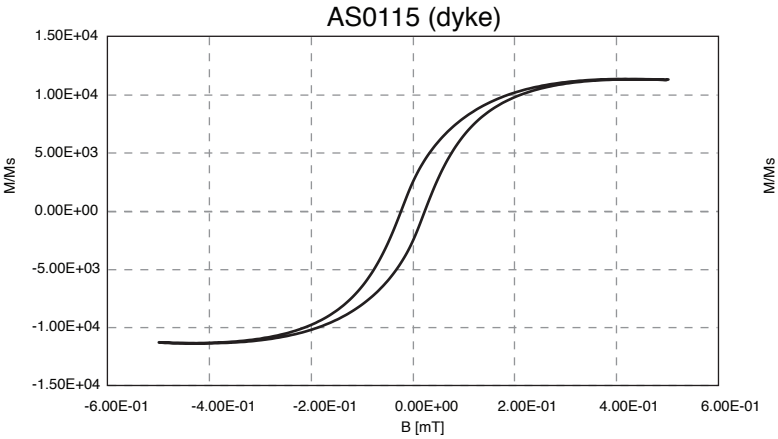

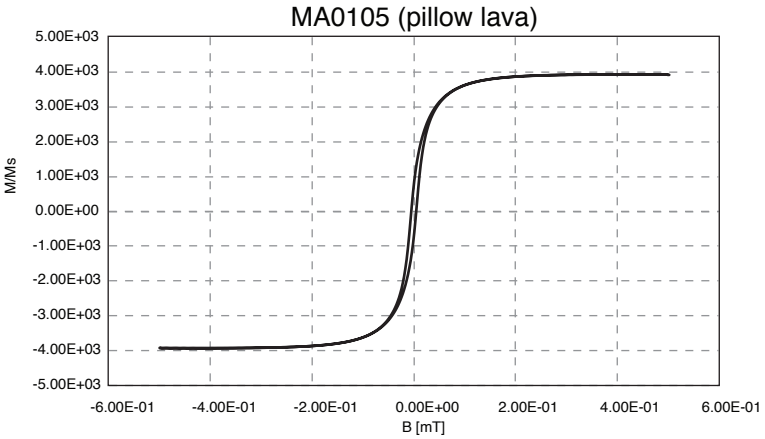

Figure 4
Click here to download Figure: Figure_4_Photomicrographs_small.pdf

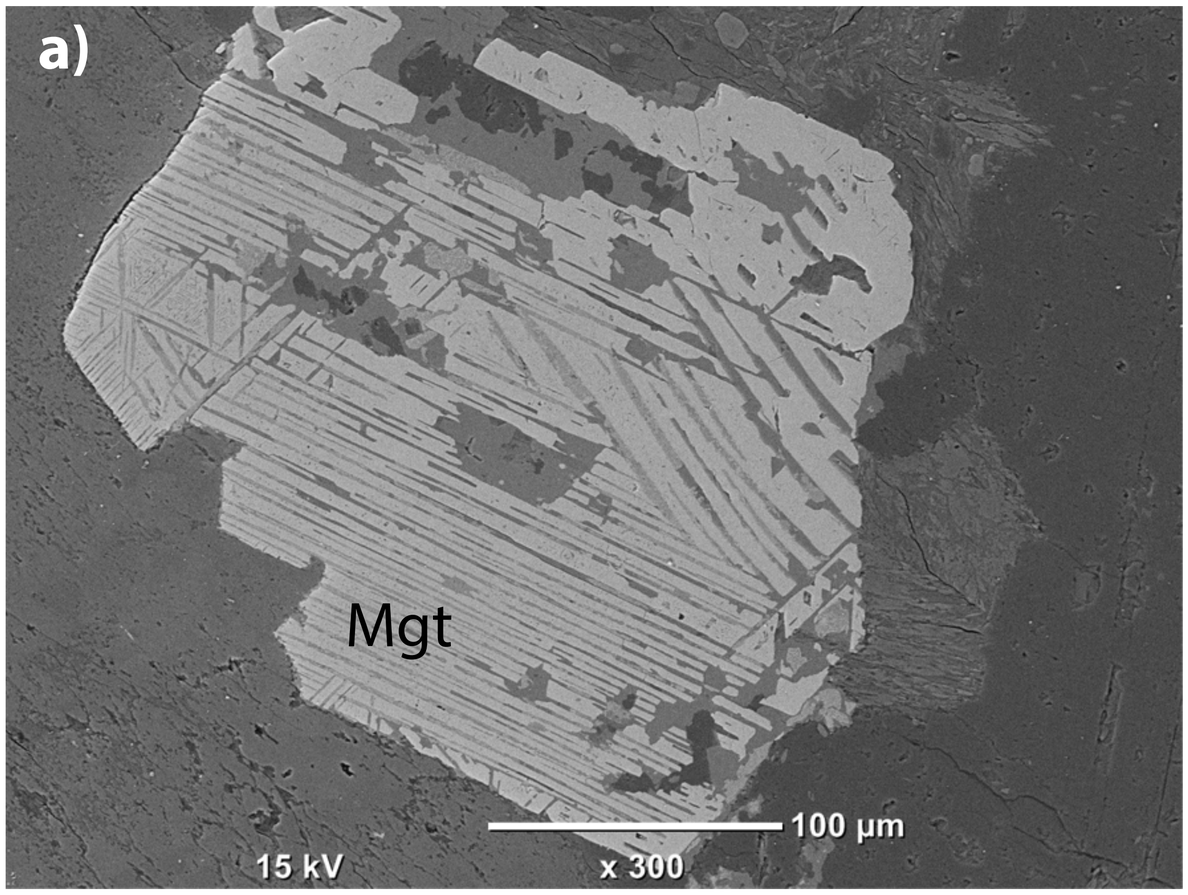

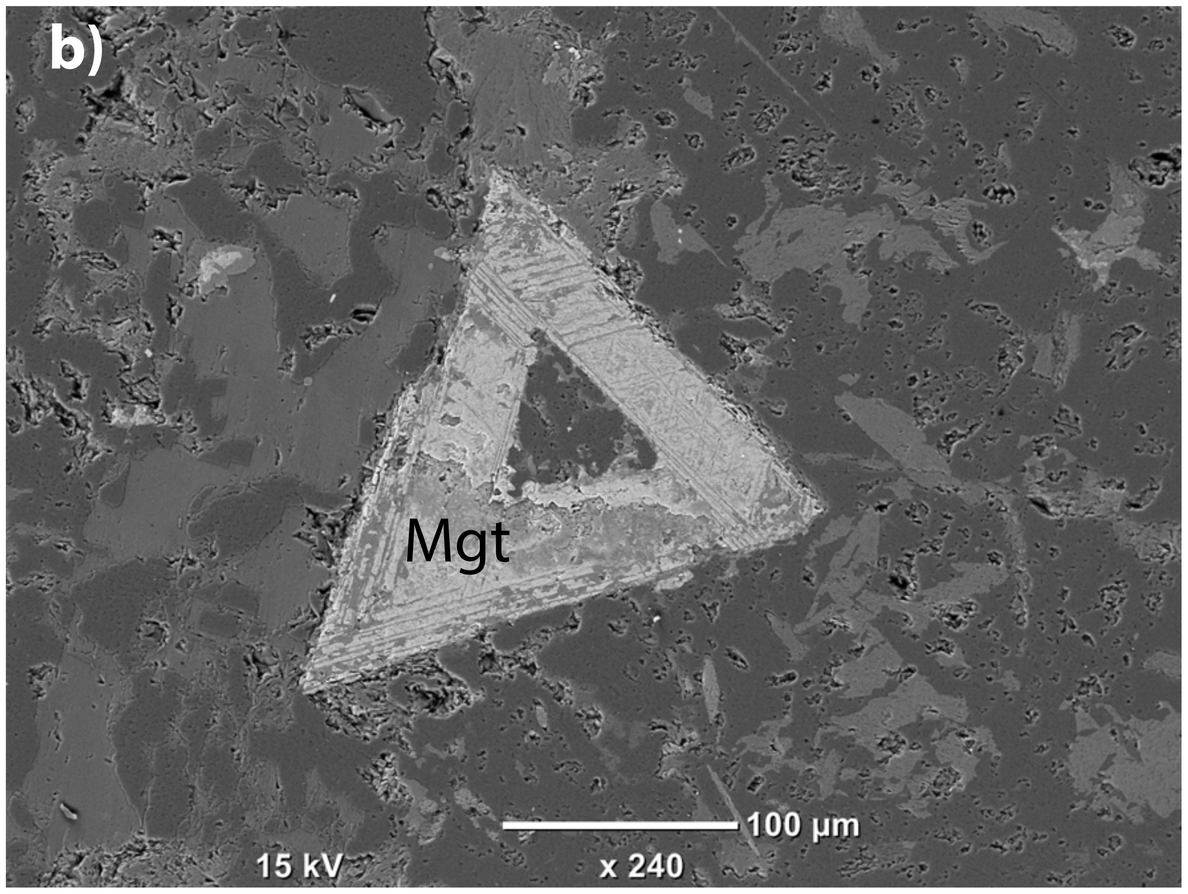

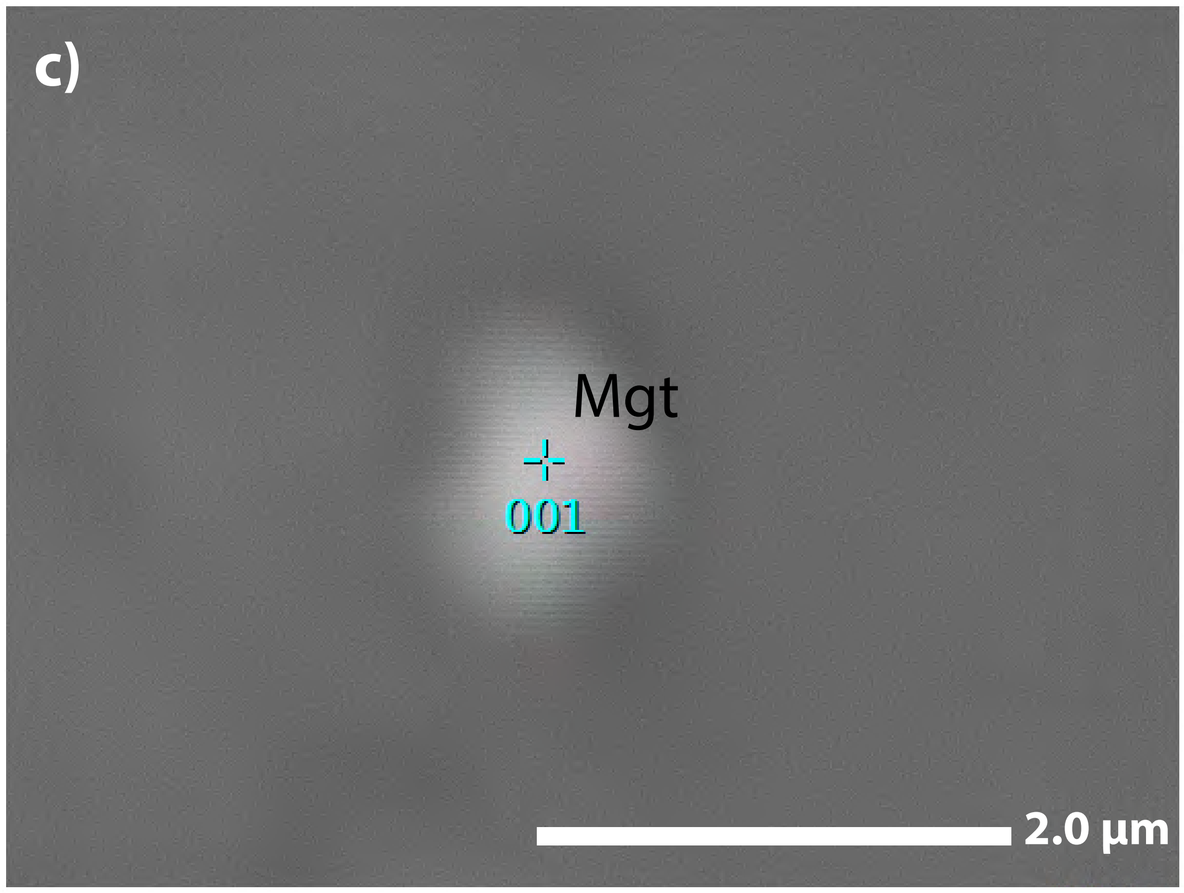

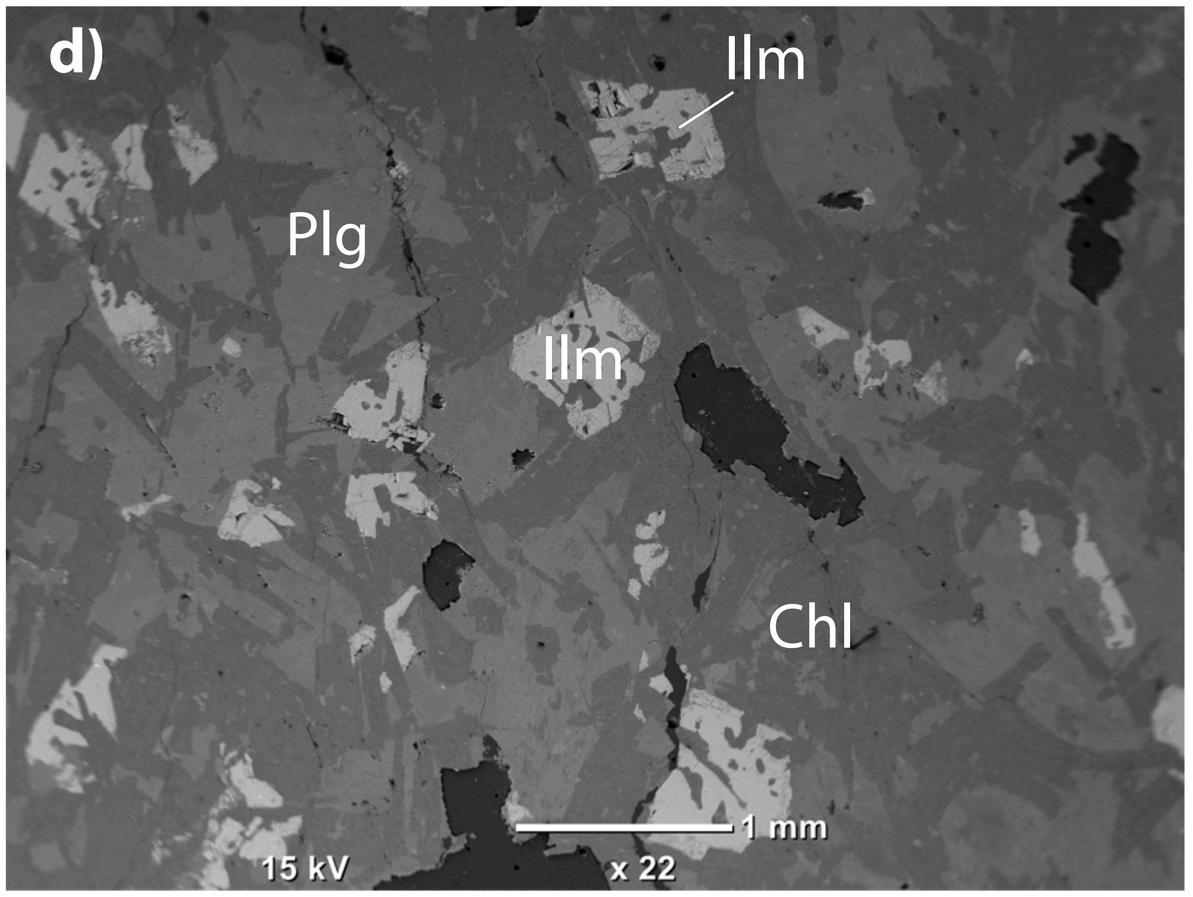

Figure 5

Click here to download Figure: Figure_5 Zijderveld Diagrams.pdf

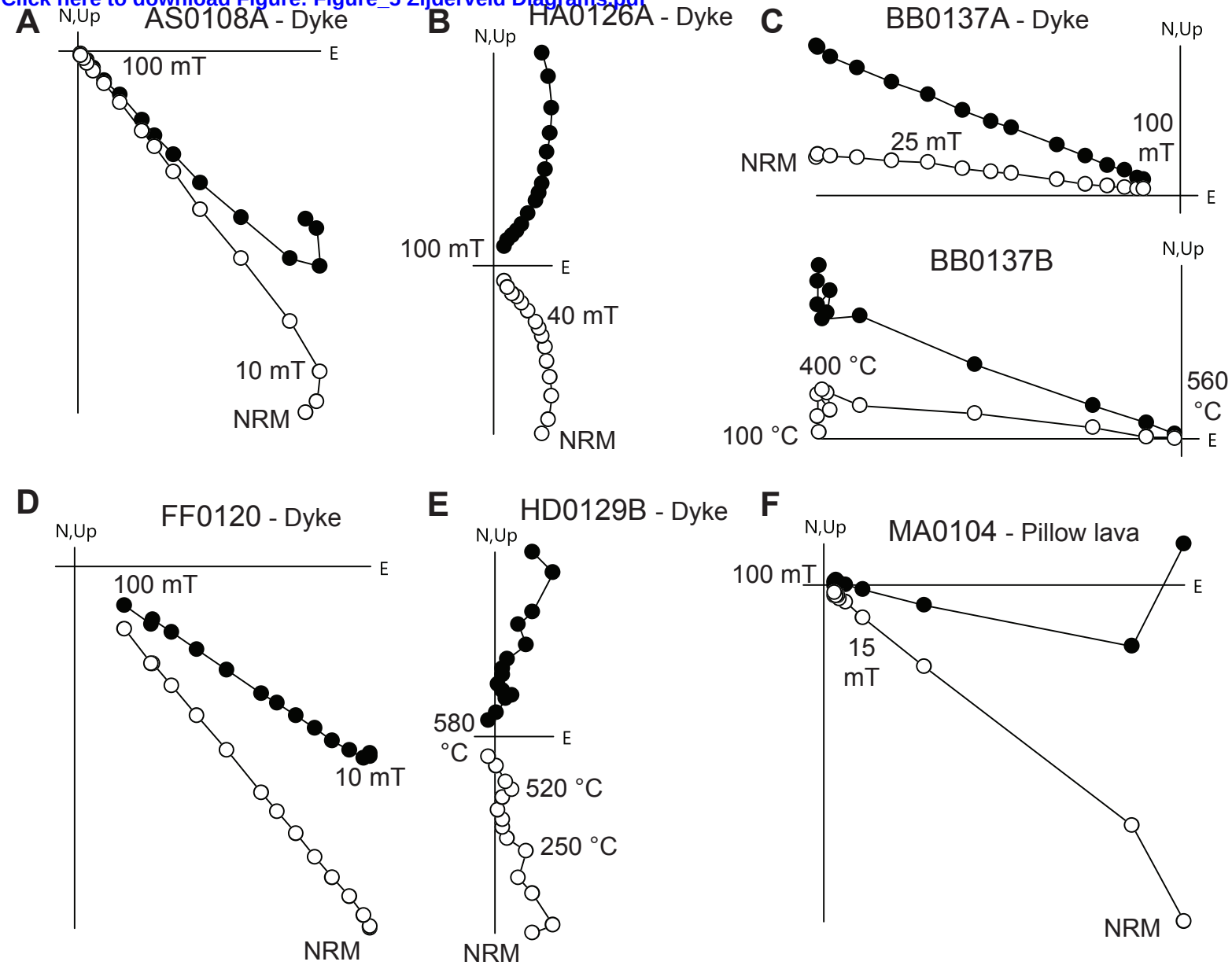

Figure 6

Click here to download Figure: Figure_6_ChRM_VGP.pdf

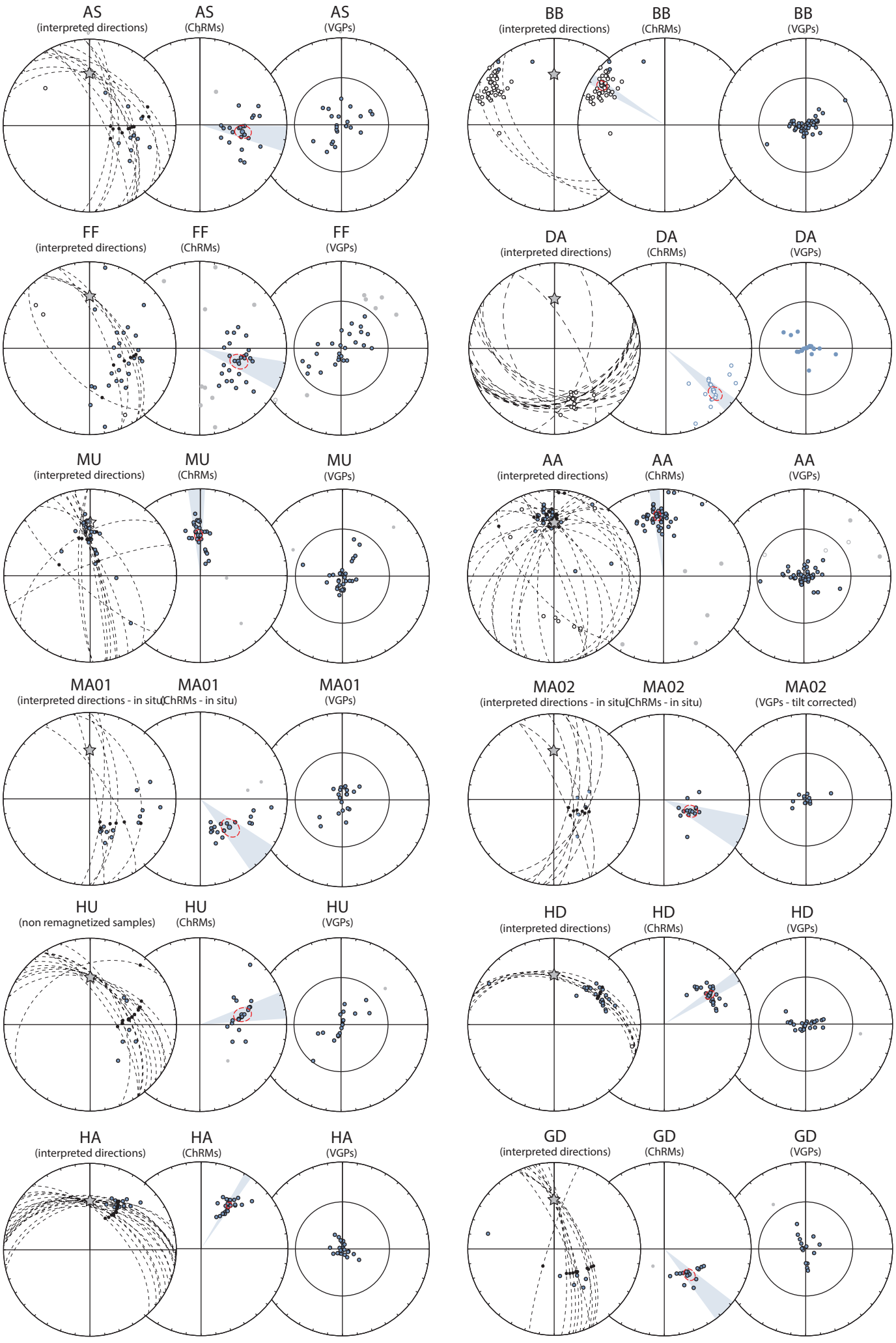

Figure 7

Click here to download Figure: Figure_7_NTR_Results.pdf

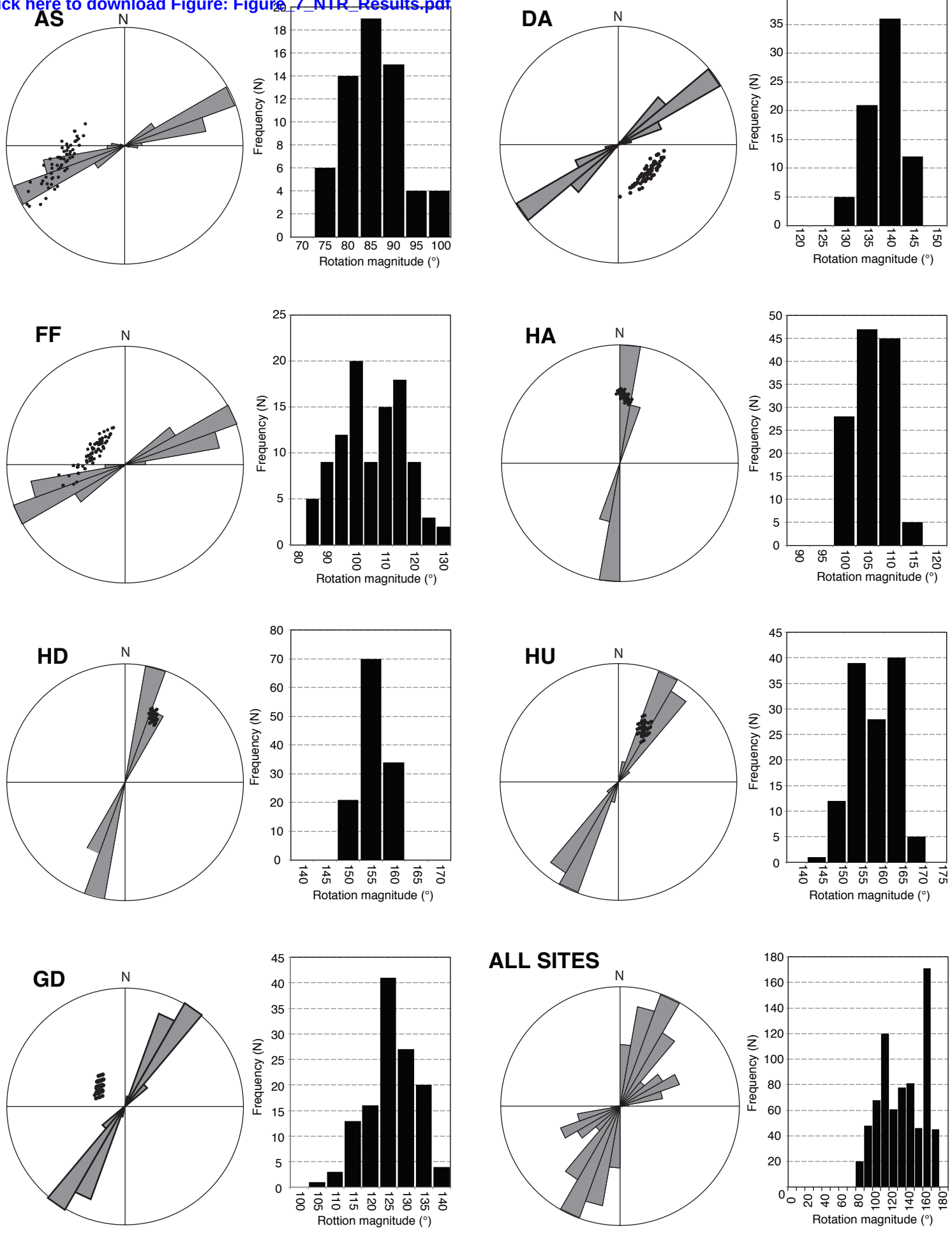

Figure 8

Click here to download Figure: Figure_8_Reconstruction_small.pdf

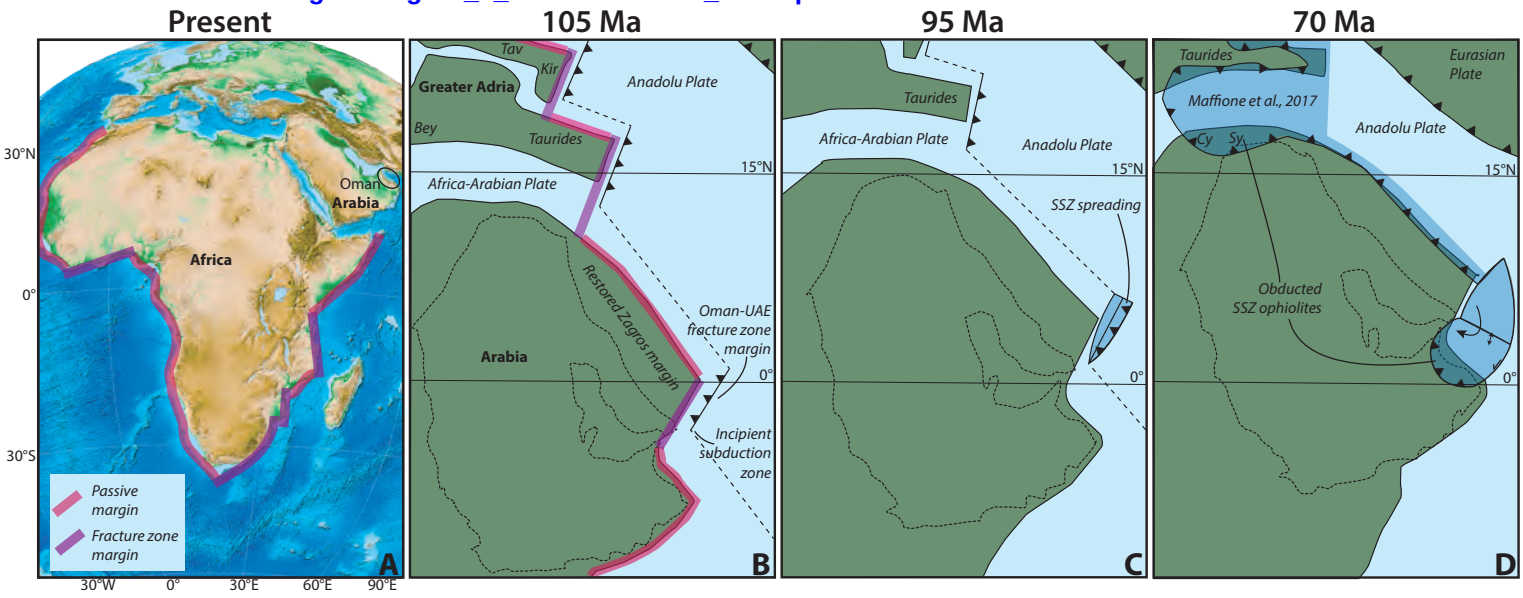

Figure 1 (high-resolution)

Click here to download Figure (high-resolution): Figure_1_Geological_Map.pdf

Figure 2 (high-resolution)

Click here to download Figure (high-resolution): Figure_2_Thermomag.pdf

Figure 4 (high-resolution)

Click here to download Figure (high-resolution): Figure_4_Photomicrographs.pdf

Figure 8 (high-resolution)

Click here to download Figure (high-resolution): Figure_8_Reconstruction.pdf

Table 1

Click here to download Table: Table 1.docx

Table 1. Paleomagnetic results from the Oman Ophiolite.

Site	Lithology	Lat (N)	Long (E)	Dip dir.	Dip	δDipDir (N meas.)	ChRM interpr.	n/N	D	ΔDx	I	ΔIx	K	A_{95}	A_{95min}	A_{95max}
AS	SD	24° 20' 09"	56° 28' 36"	235	41	5.4 (9)	12 L +12 GC	22/24	097.5	8.3	49.5	8.1	19.9	7.1	3.5	11.7
DA	SD	23° 37' 45"	56° 38' 06"	088	39	6.9 (8)	3 L +18 GC	18/21	131.2	5.2	-27.1	8.5	40.7	5.0	3.6	12.0
FF	SD	23° 49' 38"	56° 52' 46"	255	54	6.0 (6)	29 L + 6 GC	26/35	108.8	9.9	51.4	9.1	12.5	8.4	3.3	10.5
HA	SD	24° 48' 29"	56° 17' 38"	026	48	5.7 (11)	12 L + 18 GC	30/30	032.7	2.7	40.4	3.4	115.7	2.5	3.1	9.6
HD	SD	24° 13' 40"	56° 07' 53"	096	65	3.2 (11)	21 L + 7 GC	26/28	057.3	4.0	38.1	5.4	58.2	3.7	3.3	10.5
HU	SD	23° 37' 14"	57° 14' 59"	098	79	3.5 (6)	7 L + 13 GC	19/20	077.0	9.0	49.0	9.0	19.4	7.8	3.7	12.8
GD	SD	23° 59' 04"	56° 29' 52"	234	60	3.8 (9)	6 L + 11 GC	15/17	135.7	8.1	56.5	6.2	35.8	6.5	4.1	14.9
*BB	SD	23° 05' 02"	58° 10' 39"	193	77	2.3 (6)	43 L + 3 GC	46/46	302.1	3.4	-15.9	6.4	39.4	3.4	2.6	7.3
*AA	SD	22° 48' 36"	58° 34' 03"	073	71	7.5 (10)	35 L + 18 GC	48/53	354.0	3.5	31.1	5.3	39.2	3.3	2.6	7.2
*MU	SD	24° 30' 44"	56° 21' 13"	272	43	12.8 (8)	24 L + 12 GC	33/36	357.5	5.7	51.6	5.2	28.2	4.8	3.0	9.1
MA01[A]	PL	24° 20' 34"	56° 30' 27"	061	49	4.3 (6)	14 L + 6 GC	18/20	134.0	11.0	51.4	10.1	14.8	9.3	3.8	13.3
MA01[B]	PL	24° 20' 34"	56° 30' 27"	-	-	-	-	20/20	098.2	6.2	18.9	11.2	29.8	6.1	3.6	12.4
MA02[A]	PL	24° 20' 34"	56° 30' 27"	057	58	4.4 (6)	5 L + 8 GC	13/13	112.7	11.6	62.6	6.8	25.9	8.3	4.3	16.3
MA02[B]	PL	24° 20' 34"	56° 30' 27"	-	-	-	-	13/13	086.6	5.1	11.4	9.9	66.9	5.1	4.3	16.3
MA01/02[A]	PL	24° 20' 34"	56° 30' 27"	-	-	-	19 L + 14 GC	32/33	124.7	9.2	56.5	7.0	13.1	7.3	3.0	9.2
MA01/02[B]	PL	24° 20' 34"	56° 30' 27"	-	-	-	-	33/33	093.4	4.5	15.9	8.5	32.0	4.5	3.0	9.1

- Potentially remagnetized sites. [A] In situ directions. [B] Tilt corrected directions. Lithologies are sheeted dykes (SD) and pillow lavas (PL). δDipDir is the 95% confidence around the mean pole to dyke measured in the field. (N meas.) is the number of dykes measured in the field to calculate the mean direction. ChRM interpretation has used best-fit lines (L) and great circles (GC) fitting. n/N is the number of specimens used in the statistics over the total number of analysed samples. D, dDx, I, dIx are declination and associated error, and inclination and associated error. α_{95} = semiangle of the 95% cone of confidence around the site-mean ChRM direction (Fisher, 1957). K is Fisher's precision parameter relative to the ChRMs (Fisher, 1957). A_{95} is the semiangle of the 95% cone of confidence around the mean virtual geomagnetic pole (VGP). K is Fisher's precision parameter relative to the VGPs. A_{95min} and A_{95max} are the minimum and maximum semiangle of the 95% cone of confidence expected for the given dataset by paleosecular variation.

Table 2
Click here to download Table: Table 2.docx

Table 2. Net tectonic rotation solutions from the sheeted dykes of the Oman ophiolite.

Site	Preferred Solution						Alternate Solution					
	Rotation axis		Rotation		Initial dyke		Rotation axis		Rotation		Initial dyke	
	Azimuth	Plunge	Magnitude	Sense	Strike	Dip	Azimuth	Plunge	Magnitude	Sense	Strike	Dip
AS	253.8	40.4	78.5	CW	072.6	90	054.0	11.0	105.6	CCW	107.4	90
DA	131.8	61.4	135.5	CW	055.0	90	227.8	32.5	157.3	CW	125.0	90
FF	287.5	65.3	97.4	CW	070.8	90	246.1	11.2	089.3	CW	109.2	90
HA	003.9	42.8	103.5	CW	007.9	90	026.8	14.5	80.9	CCW	170.6	90
HD	023.1	39.3	153.1	CW	018.5	90	229.8	35.5	53.8	CW	161.5	90
HU	025.2	48.4	156.7	CW	029.4	90	247.7	37.2	65.7	CW	150.6	90
GD	309.1	67.6	123.6	CW	031.5	90	068.1	16.3	108.1	CCW	148.5	90
AA*	356.0	25.8	155.9	CW	179.2	90	022.5	35.5	27.1	CCW	000.8	90
MU**	324.5	29.5	57.2	CW	144.5	90	002.3	36.7	160.7	CCW	035.5	90
BB**	207.6	49.5	70.7	CCW	164.7	90	329.0	5.3	172.3	CCW	015.3	90

* Unreliable solution (see text). ** No preferred solution (both solutions are discarded). Results of the net tectonic rotation analysis (Allerton and Vine, 1987) showing the calculated values for the azimuth and plunge of the rotation axis, rotation magnitude and sense, and restored dyke strike and plunge. Reference direction used: D = 000°, I = 21.5° ± 6.6°. In situ dyke orientations and associated uncertainties used for the analysis are in Table 1. Two sets of solutions have been obtained at each site and identified as “preferred” (the one used for the tectonic interpretation) and “alternate” (the one discarded).

Supplementary material for online publication only

Click here to download Supplementary material for online publication only: Figure_S1_Reference_Dir_NTR.pdf

Supplementary material for online publication only

Click here to download Supplementary material for online publication only: Figure_S1_Reference_Direction.pdf